


 Cite this: *RSC Adv.*, 2025, **15**, 19043

## Amide linked chalcone derivatives, a promising class of compounds with versatile biological effects

 Omar Alshazly,<sup>1D</sup>\*<sup>ab</sup> Gamal El-Din A. Abuo-Rahma,<sup>1D</sup>\*<sup>bc</sup>  
 Mamdouh F. A. Mohamed<sup>1D</sup><sup>ad</sup> and Mohamed Abdel-Aziz<sup>b</sup>

Chalcone-linked acetamide derivatives represent a unique class of compounds with a broad spectrum of biological activities. Various synthetic methods for chalcones are reviewed, emphasizing their efficiency. These derivatives exhibited potent antiproliferative properties, functioning as inhibitors of key targets such as EGFR, topoisomerase I and II, ABCG2, caspase proteins, and histone deacetylase (HDAC), as well as inhibiting tubulin polymerization. The structure–activity relationships (SAR) pertinent to their anticancer activity are elucidated. In addition to their antiproliferative effects, these compounds display significant antimicrobial activities against a variety of bacterial and fungal pathogens. Their antiviral potential is also highlighted, with capabilities to inhibit critical viral enzymes and pathways. The antiprotozoal properties of chalcone-linked acetamide derivatives underscore their efficacy against protozoan infections. Furthermore, these derivatives possess strong anti-inflammatory and antioxidant activities, contributing to their overall therapeutic potential. By exploring these diverse biological activities, these compounds present significant opportunities for the development of novel therapeutic agents overcoming various medical challenges.

 Received 4th February 2025  
 Accepted 29th May 2025

DOI: 10.1039/d5ra00834d

[rsc.li/rsc-advances](http://rsc.li/rsc-advances)

## 1 Introduction

Chalcones, also known as 1,3-diphenylpropan-1-ones, serve as the initial intermediate structures in the biosynthesis of all flavonoids. These open-chain flavonoids consist of two aromatic rings (A and B) connected by a three-carbon  $\alpha$ ,  $\beta$ -unsaturated carbonyl system (Fig. 1).<sup>1,2</sup>

Many natural chalcones exhibit multiple hydroxyl groups on their aromatic rings. Typically, hydroxyl groups are found at the C2', C4', and/or C6' positions in the A-ring. The B-ring usually contains a hydroxyl group at the C4 position. Chalcones lacking an oxygen at the 2'-position are known as retrochalcones. Prenyl and methoxyl groups are commonly found as substituents in natural chalcones.<sup>1,3</sup>

These small molecular structures possess Michael acceptor features, enabling chalcones to interact with various biological molecules, facilitating their binding and reactivity. Consequently, chalcones demonstrate a wide range of biological activities encompassing anticancer, anti-inflammatory, antibacterial, antituberculosis, antidiabetic effects, antioxidant

capabilities, antimicrobial and antiviral, antimalarial, neuroprotective effects, among others.<sup>4–13</sup> Interestingly, a single chalcone compound can manifest multiple types of bioactivity. For instance, isoliquiritigenin (Fig. 2a) exhibits anticancer, cancer-chemo-preventive, antioxidant, and anti-inflammatory activities.<sup>14,15</sup> Similarly, xanthohumol (Fig. 2b) demonstrates anti-HIV-1, antibacterial, and anticancer effects.<sup>16</sup> It is worth

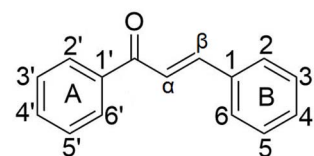
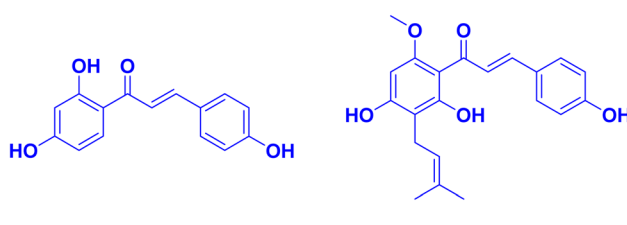


Fig. 1 Chalcones scaffold.



a) Isoliquiritigenin

b) Xanthohumol

Fig. 2 Examples of natural bioactive chalcones; (a) isoliquiritigenin, (b) xanthohumol.

<sup>a</sup>Department of Pharmaceutical Chemistry, Faculty of Pharmacy, Sohag University, 82524 Sohag, Egypt

<sup>b</sup>Department of Medicinal Chemistry, Faculty of Pharmacy, Minia University, 61519 Minia, Egypt. E-mail: gamalaburahma@yahoo.com; Tel: +20-1003069431

<sup>c</sup>Department of Pharmaceutical Chemistry, Faculty of Pharmacy, Deraya University, New-Minia, Egypt

<sup>d</sup>Department of Pharmaceutical Chemistry, Faculty of Pharmacy, New Valley University, New Valley, 72511, Egypt



noting that alongside the therapeutic potentials of chalcones, researchers have also evaluated their potential side effects.<sup>17,18</sup> Notably, Xing *et al.*<sup>19</sup> discovered a hepatotoxic risk associated with a specific type of chalcone, emphasizing the importance of further comprehensive investigation in this area.

Amide group are not only common structural motifs in biologically active molecules but also play a critical role in modulating physicochemical properties such as solubility, lipophilicity, and metabolic stability.<sup>20,21</sup> More importantly, the amide moiety contributes significantly to molecular recognition through various non-covalent interactions, including hydrogen bonding and dipole-dipole interactions, which are essential for enhancing binding affinity and specificity toward biological targets.<sup>22</sup>

By integrating an amide functionality into the chalcone structure, it is possible to synergistically combine the electrophilic Michael acceptor character of chalcones with the favorable binding properties of amides.<sup>10</sup> This hybrid design strategy is expected to enhance target interaction, improve bioavailability, and potentially lead to compounds with superior pharmacological profiles.<sup>23</sup> Thus, chalcone-linked acetamide derivatives represent a promising class of compounds for drug discovery and development.<sup>24</sup>

This article present various synthetic approaches for chalcone derivatives and comprehensively review the specific biological activities associated with chalcones incorporating

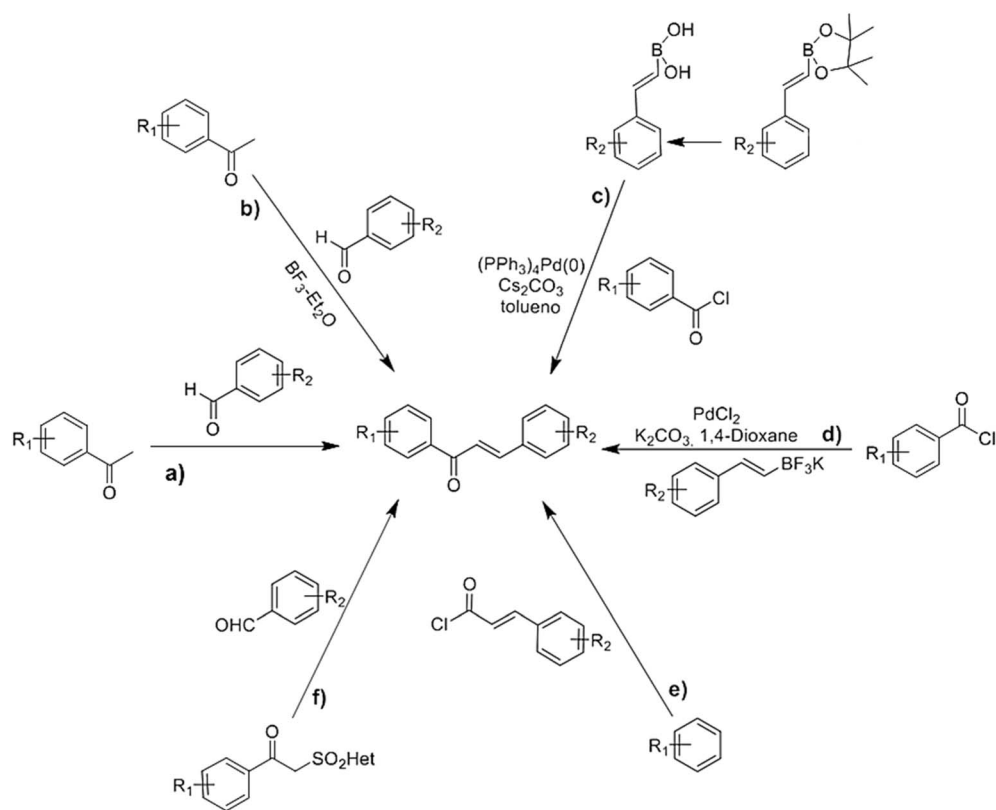
amide functionalities, with a particular focus on recent advancements and current research developments in this field.

## 2 Methods of synthesis of chalcones

Many methods have been developed for synthesizing chalcones, which are a significant class of natural products possessing diverse biological activities. Moreover, chalcones serve as precursors for the synthesis of numerous compounds. Furthermore, there has been a considerable amount of research focused on developing synthetic strategies to produce chalcones that mimic their natural counterparts, as well as synthesis of novel molecules. The following sub-sections provide an overview of the primary methodologies employed for this purpose (Scheme 1).

### 2.1 Synthesis of chalcones by Claisen–Schmidt reaction

The Claisen–Schmidt condensation is a widely used method for synthesizing chalcones, involving the condensation of acetophenone and benzaldehyde derivatives to form  $\alpha,\beta$ -unsaturated ketones, linking aromatic rings A and B (Scheme 1a).<sup>25</sup> The reaction proceeds through the nucleophilic addition of the carbanion, derived from the aryl ketones to the carbonyl carbon of the aromatic aldehydes, the Claisen–Schmidt reaction is typically carried out in the presence of an aqueous, methanolic



**Scheme 1** Different methods of chalcones synthesis. (a) Claisen–Schmidt reaction; (b) using boron trifluoride-etherate; (c) via Suzuki coupling reaction; (d) direct cross-coupling reaction; (e) Friedel–Crafts acylation; (f) Julia–Kocienski olefination.  $R_1$  and  $R_2$  = electron donating or electron withdrawing groups.



or ethanolic alkaline solution, at room temperature or at reflux for several hours.<sup>26</sup> Moreover, microwave (MW) irradiation has been effectively employed. This method involves the condensation of acetophenone and benzaldehyde derivatives in the presence of anhydrous potassium carbonate under free-solvent conditions. Anhydrous  $K_2CO_3$  is a cost-effective, non-toxic, and user-friendly alternative to stronger bases like NaOH or KOH, which are typically used in traditional Claisen–Schmidt reactions but can be harmful, toxic, and environmentally polluting. Khan, S. A., *et al.*<sup>27</sup> successfully applied this methodology to synthesize various chalcone derivatives with high yields.

## 2.2 Synthesis of chalcones using borontrifluoride etherate

In 2007, Narendar and Reddy developed a method utilizing borontrifluoride etherate for the synthesis of diverse chalcones. Instead of the traditional base-catalyzed Claisen–Schmidt reaction, this method involves the reaction between various substituted acetophenones and aromatic aldehydes using  $BF_3$ – $Et_2O$  as a catalyst, yielding chalcones within a timeframe of 15–150 minutes (Scheme 1b).<sup>28</sup> Compared to the conventional Claisen–Schmidt condensation reactions employing KOH or NaOH, this method offers several advantages. These include high yields, simplified work-up procedures, shorter reaction times, absence of side reactions, and compatibility with sensitive functional groups such as amides and esters.<sup>28</sup>

## 2.3 Synthesis of chalcones by direct cross-coupling reaction

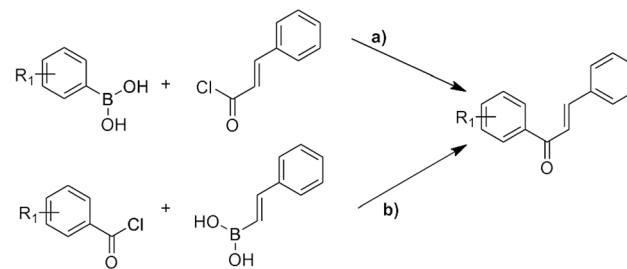
The direct cross-coupling reaction involves the coupling of benzoyl chlorides and potassium styryltrifluoroborates using a palladium-catalyzed system under microwave (MW) irradiation. This method enables the one-pot synthesis of  $\alpha,\beta$ -unsaturated aromatic ketones. Al-Masum *et al.*<sup>29</sup> were the first to utilize this approach for the synthesis of several chalcones, employing 1,4-dioxane as a solvent and  $K_2CO_3$  as a base (Scheme 1d). Despite 1,4-dioxane being a non-polar solvent typically not used in MW irradiation reactions, its polarizability due to the presence of two oxygen atoms and relatively high boiling point is advantageous for facilitating the desired cross-coupling reaction. This process offers notable advantages, including the non-toxicity, ease of preparation, and ease of removal of potassium styryltrifluoroborates.

## 2.4 Synthesis of chalcones by Friedel–Crafts acylation

Chalcones can be synthesized through a direct Friedel–Crafts acylation reaction involving a phenol. In this reaction, the phenol serves as the precursor for the formation of the chalcone's A-ring, while the acylating agent contributes to the formation of both the B-ring and the three-carbon bridge connecting rings A and B (Scheme 1e). Various catalysts have been employed for this reaction, including anhydrous aluminum chloride,<sup>30</sup> aluminum bromide,<sup>31</sup> and chiral phosphoric acids.<sup>32</sup>

## 2.5 Synthesis of chalcones by Julia–Kocienski olefination

The approach described in this method plays a pioneering role in the synthesis of chalcones and flavanones. It involves the



Scheme 2 Method of synthesis of chalcones via Suzuki coupling reaction.

condensation of aldehydes with 2-(benzo[d]thiazol-2-ylsulfonyl)-1-phenylethanones, which are reagents developed for Julia–Kocienski olefination. This reaction is carried out in the presence of a base (Scheme 1f). The resulting product is obtained in good yields.<sup>33</sup>

## 2.6 Synthesis of chalcones by Suzuki coupling reaction

The Suzuki reaction is a valuable tool utilized for the formation of carbon–carbon (C–C) bonds. It involves the coupling of organoboron compounds with organic halides or triflates, catalyzed by palladium in the presence of a base (Scheme 1c). This reaction has found widespread application in the synthesis of various compounds, including chalcones.<sup>34</sup>

In 2003, Eddarir *et al.*<sup>35</sup> introduced a method for synthesizing chalcones through the Suzuki coupling reaction. This method involves the coupling of cinnamoyl chlorides with phenylboronic acids (Scheme 2a) or the coupling of benzoyl chlorides with phenylvinylboronic acid (Scheme 2b).

## 2.7 Synthesis of chalcones by grinding technique

By utilizing the grinding technique, certain chalcone derivatives have been successfully synthesized. This method involves the reaction between substituted 2-acetyl-1-naphthol and various substituted benzaldehydes in the presence of a base. Notably, this reaction does not require a catalyst, making it non-hazardous and environmentally safer. Furthermore, it offers the advantage of yielding excellent results in a short reaction time, leading to high product yields.<sup>26</sup>

## 3 Antiproliferative properties

The documentation of the antiproliferative activity of acetamido chalcones is increasing. Many research groups synthesized or modified natural chalcones that possess antiproliferative activity. Chalcones showed an ability of targeting multiple cellular molecules, such as mouse double minute 2 MDM2/p53,<sup>36</sup> tubulin,<sup>37</sup> nuclear factor kappa-light-chain-enhancer of activated B cells NF- $\kappa$ B,<sup>38</sup> vascular endothelial factor VEGF, VEGFR-2 kinase,<sup>39</sup> hypoxia-inducible factor-1 HIF-1,<sup>40</sup> matrix metalloproteinase MMP-2/9 (ref. 41) and P-glycoprotein P-gp<sup>42</sup>/ multidrug resistance-associated protein MRP1 (ref. 43)/breast cancer-resistance protein BCRP.<sup>44</sup> Which indicates that chalcones can act as an anticancer *via* tumor cell apoptosis



induction, microtubule polymerization, anti-inflammatory, antiangiogenesis.<sup>45</sup> These characters made chalcones highly desirable as fundamental constituents for developing agents that target cancer molecules.

### 3.1 Chalcones as EGFR inhibitors

EGFR (epidermal growth factor receptor) is a protein involved in cell growth and survival. However, in certain cancers, EGFR becomes overactive or mutated, leading to uncontrolled cell growth.<sup>46</sup> Targeting EGFR has emerged as an important strategy in anticancer treatment. EGFR inhibitors, such as small molecule tyrosine kinase inhibitors (TKIs) or monoclonal antibodies, are designed to block EGFR activity and its downstream signaling pathways.<sup>47</sup> Small molecule TKIs, like erlotinib or osimertinib (Fig. 3), inhibit the intracellular domain of EGFR, preventing the phosphorylation of downstream molecules.<sup>48</sup> Monoclonal antibodies, such as cetuximab or panitumumab, bind to the extracellular domain, blocking ligand binding and receptor activation.<sup>49</sup> By inhibiting EGFR, these drugs suppress cell proliferation and survival, induce apoptosis, and inhibit tumor angiogenesis. EGFR inhibitors can also modulate the immune response against cancer cells, enhancing immune recognition and promoting antitumor immune responses.<sup>50</sup> However, the effectiveness of EGFR-targeted therapies can vary depending on cancer type and the presence of specific EGFR mutations. Resistance to EGFR inhibitors can also develop, necessitating combination therapies and personalized treatment approaches.<sup>51</sup>

A series of quinoline/chalcone hybrids containing 1,2,4-triazole moiety was tested by ref. 52, for its antiproliferative activities. All of the selected compounds were tested in four cancer cell lines: the pancreatic cancer cell line Panc-1, the breast cancer cell line MCF-7, the colon cancer cell line HT-29,

and the epithelial line cancer cell A-549. The five most active compounds were 1, 2, 3, 4, and 5 (Fig. 4). Among these compounds, 2 exhibited the highest activity against cancer cell growth, with a  $GI_{50}$  of  $3.325 \mu\text{M}$ . Compound 2, which has an allyl-triazole backbone, displayed the highest anticancer potential. On the other hand, compound 1, which has the same substitution pattern as 2 but a different phenyltriazole moiety, showed almost 2.5 times lower activity than 2. These findings suggest that all compounds with an allyl-triazole backbone were better inhibitors of cancer cell growth compared to derivatives with the same substitutions but a different phenyltriazole backbone, and the presence of trimethoxy phenyl at the chalcone moiety showed increase in the antiproliferative activity. All investigated compounds 1, 2, 3, 4, and 5 exhibited inhibitions of EGFR with  $IC_{50}$  ranging from  $1.3$  to  $4.8 \mu\text{M}$  in comparison to the positive control erlotinib ( $IC_{50} = 0.08 \pm 0.04 \mu\text{M}$ ). This study demonstrates that these compounds are effective EGFR inhibitors.

Fathi and coworkers<sup>53</sup> synthesized series of chalcone/1,3,4-oxadiazole derivatives in order to study the effect of these derivatives against different cancer cell lines. The compounds exhibited promising anticancer activities particularly leukemia cell lines compounds, 6, 7, 8, and 9 (Fig. 5) were the most potent (mean growth inhibition% = 37.77, 27.29, 28.20, and 132.29; respectively). Compound 9 exhibited potent cytotoxic activity against most of the tested cell lines. Compounds 6, 7, 8, and 9 displayed the highest inhibitory activities against EGFR ( $IC_{50} = 0.24\text{--}2.35 \mu\text{M}$ ) as well as Src kinase ( $IC_{50} = 0.96\text{--}6.24 \mu\text{M}$ ). Out of all the derivatives, 6, 7, and 9 demonstrated the highest effectiveness in inhibiting the activity of signal transducer and activator of transcription 3 (STAT3), which indicate that the substitution of phenyl ring carrying the oxadiazole moiety showed the highest activity with the 3,4,5-trimethoxy < H < *p*-methoxy, and the most effective substitution of the chalcone phenyl ring was *p*-methoxy, as a result they found that to achieve the best possible activity, it is necessary for  $R_1$  to consist of 3,4,5-trimethoxy groups and for  $R_2$  to contain a methoxy group in the *p*-position. Therefore, in order to exhibit effective anti-cancer properties, it is ideal for either both phenyl rings to be unsubstituted or for one of the rings to contain a *p*-methoxy group, while the other ring should have 3,4,5-trimethoxy groups.

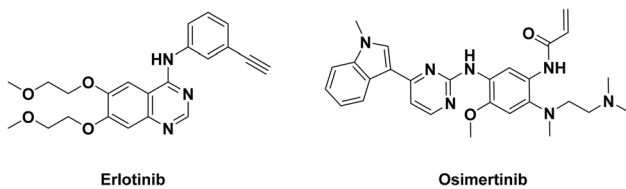


Fig. 3 EGFR inhibitors – erlotinib and osimertinib.

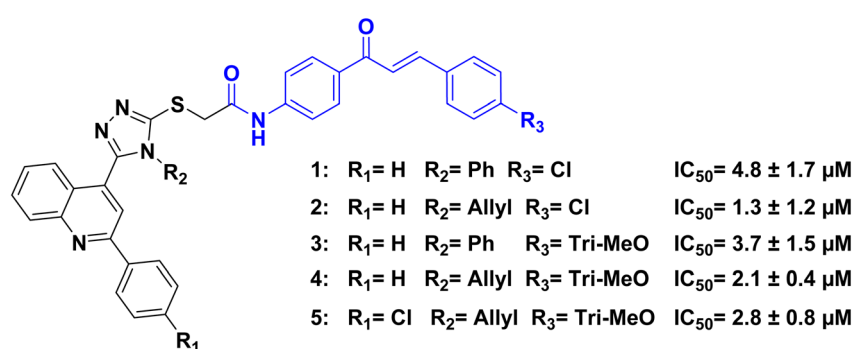


Fig. 4 Quinoline/chalcone hybrids 1–5 as EGFR inhibitors.



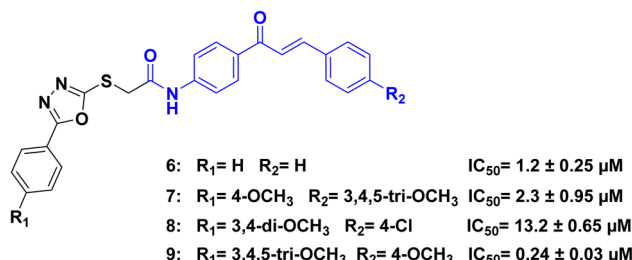


Fig. 5 Chalcone/1,3,4-oxadiazole hybrids 6–9 as EGFR inhibitors.

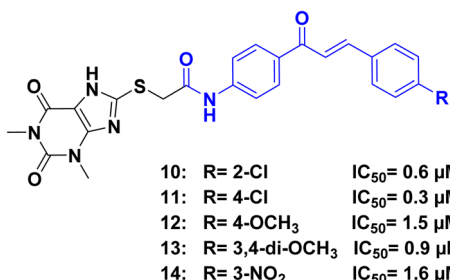


Fig. 6 Xanthine/chalcone hybrids 10–14 as EGFR inhibitors.

Abou-Zied, *et al.*<sup>54</sup> tested a series of xanthine/chalcone derivatives for possible antiproliferative activity. Compounds **10**, **11**, **12**, **13**, and **14** (Fig. 6), demonstrated strong inhibition of cancer cell growth, with  $IC_{50}$  values ranging from  $1.0 \pm 0.1$  to  $3.5 \pm 0.4$   $\mu M$  against four cancer cell lines A-549 (epithelial cancer cell line), MCF-7 (breast cancer cell line), Panc-1 (pancreas cancer cell line), and HT-29 (colon cancer cell line). In comparison, doxorubicin exhibited  $IC_{50}$  values ranging from  $0.90 \pm 0.62$  to  $1.41 \pm 0.58$   $\mu M$ . Compounds **11** and **14** showed the highest effectiveness in the study. To understand their anticancer mechanism, compounds **10**, **11**, **12**, **13**, and **14** were tested for their inhibition of EGFR. Compound **11** demonstrated the strongest inhibition with an  $IC_{50}$  value of  $0.3 \mu M$ , which is more potent than the reference drug staurosporine ( $IC_{50} = 0.4 \mu M$ ). The activity of the compounds can be attributed to the substitutions (R) at position 4 of the chalcone phenyl ring. Notably, among the 1,3-dimethyl xanthine series, compounds with  $NO_2$ ,  $Cl$ , and  $OCH_3$  groups on the chalcone phenyl ring exhibited the highest inhibitory activity across various cell lines. Despite the differing chemical nature of the substituents, this enhanced activity may be attributed to different physicochemical nature of the chalcone/xanthine hybrids which could result in improved cell membrane permeability of these hybrids and lead to this enhanced antiproliferative activity.

Hisham *et al.*<sup>55</sup> synthesized a series of hybrid molecules consisting of quinazoline-4-one and chalcone parts as EGFR enzyme inhibitors with antiproliferative activity against cancer cells. The target compounds were synthesized and tested *in vitro* against various cancer cell lines, the EGFR enzyme, and the BRAF enzyme which is a serine/threonine-protein kinase involved in the MAPK signaling pathway, regulating cell growth

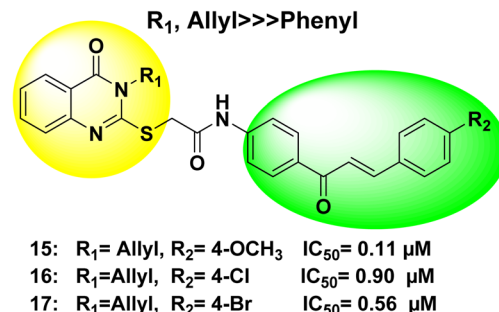
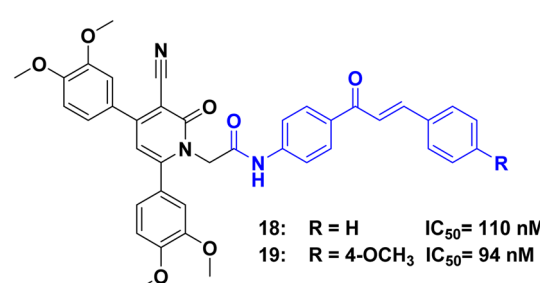
R<sub>2</sub>, Methoxy > 4-Br > 4-Cl > 3,4-dimethoxy > H >> CH<sub>3</sub>

Fig. 7 Structure–activity relationship of the target compounds (15–17).

and differentiation. Out of the synthesized compounds, three showed the greatest antiproliferative activity (**15**, **16**, and **17**) and were the most potent inhibitors of the EGFR enzyme with  $IC_{50} = 0.11$ ,  $0.90$ , and  $0.56 \mu M$ , respectively comparable to the positive control erlotinib ( $IC_{50} = 0.08 \mu M$ ). The order of effectiveness for the (R<sub>2</sub>) substituent was 4-methoxy > 4-Br > 4-Cl > 3,4-dimethoxy > H > CH<sub>3</sub> (Fig. 7).

Hybrids of cyanopyridine/chalcone acetamide derivatives were synthesized by Abou-Zied *et al.*<sup>56</sup> These derivatives were designed to inhibit EGFR enzyme. Compounds **18**, and **19** (Fig. 8) exhibited strong inhibition of cancer cell growth in multiple cell lines, outperforming the reference compound doxorubicin. These compounds were found to have a dual inhibitory effect on both EGFR and BRAFV600E (which is a mutant form of the BRAF enzyme with a V600E substitution) based on *in vitro* studies. Compounds **8**, **12**, and **13** demonstrated significant inhibition of EGFR protein, with  $IC_{50}$  values of  $110$  and  $94 \text{ nM}$ , respectively, in the synthesized compounds. The study revealed that the specific atoms or arrangements in the aryl R distal chalcone' group affected potency, with 3,4-dimethoxy being more potent than hydrogen, 4-bromo, 4-chloro, and 3,4,5-trimethoxy substitutions for compounds with the 4,6-bis(3,4-dimethoxyphenyl)pyridine core structure.

Hagar *et al.*<sup>57</sup> designed and synthesized a series of 1,3,4-oxadiazole chalcone/benzimidazole hybrids. These hybrids showed notably strong abilities to inhibit the growth of different types of cancer cells in an initial screening test. The abilities of the synthesized compounds to inhibit the growth of

Fig. 8 Cyanopyridine/chalcone hybrids **18**, and **19** as EGFR inhibitors.

cancer cells were evaluated against four human cancer cell lines: lung cancer cells (A-549), breast cancer cells (MCF-7), pancreatic cancer cells (Panc-1), and colon cancer cells (HT-29). Acetamido compounds and their acetate isostere compounds, showed promising abilities to inhibit cancer cell growth with  $IC_{50}$  values ranging from 0.80 to 2.27  $\mu\text{M}$  compared to doxorubicin ( $IC_{50}$  values ranging from 0.90 to 1.41  $\mu\text{M}$ ). The most effective compound was compound 20, with an  $IC_{50}$  value of  $1.8 \pm 0.7 \mu\text{M}$  against EGFR. This compound had the following substituents:  $R_1 = \text{methoxy}$ ,  $R_2 = \text{chlorine}$ , and  $X = \text{nitrogen}$ . The second most effective compound was 21, with an  $IC_{50}$  of  $1.9 \pm 0.8 \mu\text{M}$  against EGFR. This compound had the substituents:  $R_1 = \text{methoxy}$ ,  $R_2 = \text{chlorine}$ , and  $X = \text{oxygen}$ . The study found that the acetamide molecular group connecting the benzimidazole, oxadiazole unit, and chalcone showed better activity than the acetate linker. Regarding the substitution pattern on the phenyl ring of the chalcone unit, in both the acetamide and ester derivatives, the order of preference was: 4-methoxy > 4-chlorine > 3,4-dimethoxy > 3,4,5-trimethoxy > unsubstituted hydrogen, as shown in (Fig. 9).

Abdelbasset *et al.*<sup>58</sup> synthesized thienoquinoline carboxamide–chalcone derivatives by cyclizing acylated chalcones with 2-mercaptopquinoline-3-carbaldehyde. These thienoquinolines demonstrated promising antiproliferative effects across all tested cell lines and exhibited significant activity as inhibitors of EGFR. Among the series, compound 22 (Fig. 10) exhibited significant antiproliferative activities with  $IC_{50}$  values of 1.0, 0.9, 0.9 and 1.2  $\mu\text{M}$  against the colon cancer cell line HT-29, pancreatic carcinoma cell line paca-2, lung cancer cell line H-460 and human pancreatic cancer cell line Panc-1, respectively. Compound 23 exhibited the highest antiproliferative activity among all the tested thienoquinolines, and its activities were comparable to those of erlotinib against all the tested cancer cell lines. Moreover, thienoquinoline 23 showed  $IC_{50}$

values of 0.5, 0.8, 0.2 and 1.0  $\mu\text{M}$  against the colon cancer cell line HT-29, pancreatic carcinoma cell line paca-2, lung cancer cell line H-460 and human pancreas cancer cell line Panc-1, respectively. Furthermore, compound 23 was found to influence pre G1 apoptosis and induce cell cycle arrest at the G2/M phase.

Maghraby *et al.*<sup>59</sup> synthesized a series of 1,2,3-triazole/chalcone hybrids, and evaluated for the antiproliferative activity of these hybrids against four different cancer cell lines A-549 (epithelial cancer cell line), MCF-7 (breast cancer cell line), Panc-1 (pancreas cancer cell line), and HT-29 (colon cancer cell line), with doxorubicin used as a reference compound. Among the hybrids tested, multiple compounds demonstrated the remarkable antiproliferative activity, with  $IC_{50}$  values ranging from 0.95 to 1.80  $\mu\text{M}$ , more potent than doxorubicin ( $IC_{50}$  1.14  $\mu\text{M}$ ). Specifically, compound 24 (Fig. 11) showed the most potent antiproliferative effect and was also a highly effective inhibitor of EGFR, with an  $IC_{50}$  of  $0.09 \pm 0.05 \mu\text{M}$ , comparable to the reference drug erlotinib ( $IC_{50} = 0.05 \pm 0.03 \mu\text{M}$ ). Furthermore, compound 24 exhibited modest inhibitory activity against BRAF, with an  $IC_{50}$  of  $0.90 \pm 0.10 \mu\text{M}$ . Molecular docking studies provided insights into the strong interactions of the inhibitors with the EGFR-TK domain. Additionally, cell cycle analysis revealed that compound 24 induced cell cycle arrest at the G1 transition phase.

The studies on amide linked chalcone based EGFR inhibitors reveal several common trends that enhance their potency. Substitutions on the chalcone phenyl ring, particularly with methoxy groups (especially in the 4-position), significantly improve EGFR inhibition, with 3,4,5-trimethoxy or *p*-methoxy substitutions proving most effective. Additionally, the inclusion of heterocyclic moieties, such as triazole, oxadiazole, quinazoline, xanthine, and thienoquinoline, boosts binding affinity and enhances potency, with quinoline/chalcone hybrids particularly

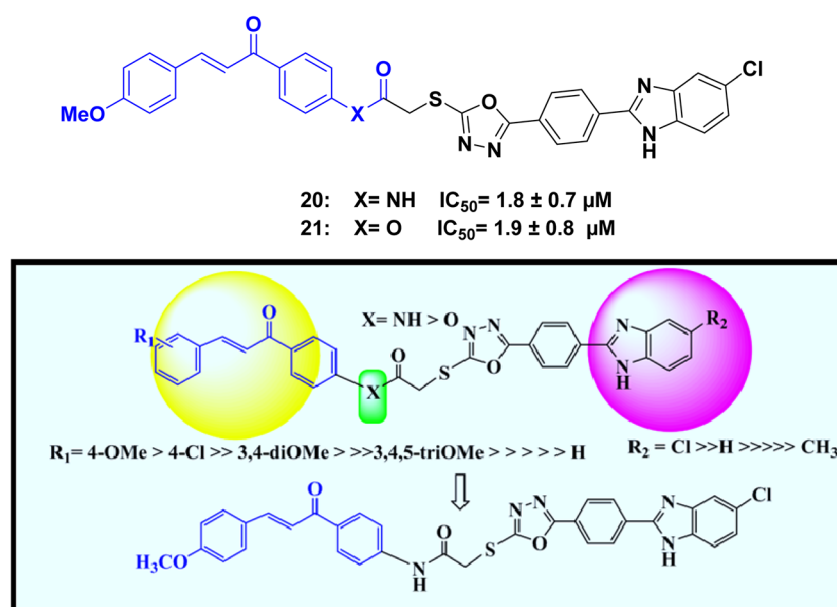


Fig. 9 Structure–activity relationship of the target compounds (20–21).



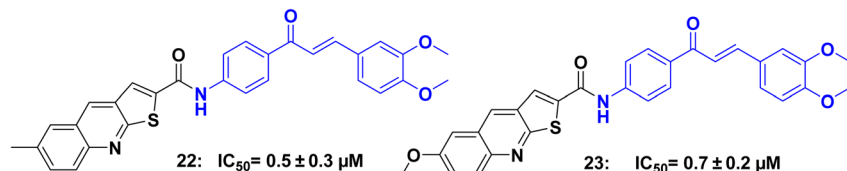


Fig. 10 Thienoquinoline/chalcone hybrids 22, and 23 as EGFR inhibitors.

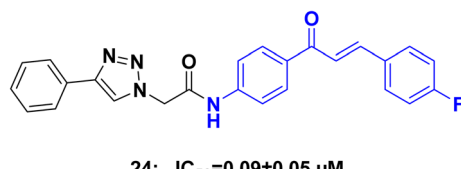


Fig. 11 1,2,3-Triazole/chalcone acetamides 24 as EGFR inhibitor.

showing strong activity. The allyl-triazole backbone also stands out as a key feature, offering higher efficacy compared to the phenyltriazole variant, emphasizing the importance of linker structure in overall compound effectiveness. These compounds demonstrated broad cell line selectivity, inhibiting cancer cell growth in pancreatic, lung, colon, and breast cancer cells, with  $IC_{50}$  values comparable to the standard EGFR inhibitor erlotinib ( $\sim 0.08 \mu M$ ), suggesting their potential as viable candidates. Moreover, several compounds exhibited dual inhibition of EGFR alongside other targets, such as BRAF and STAT3, offering a promising strategy to overcome resistance mechanisms and enhance therapeutic outcomes.

### 3.2 Topoisomerase I and II inhibitors

Certain molecules can interfere with the function of topoisomerase enzymes, which are proteins that modify DNA strands during cell activities like copying and expressing genes. There are two main topoisomerase types: topoisomerase I and II. Inhibiting topoisomerase activity can stop cell growth by disrupting DNA handling, making topoisomerase inhibitors a group of substances that prevent proliferation. Some structures exhibit antiproliferative properties through their ability to block one or both topoisomerase types, thereby hindering cell division. Researchers examine the capacity of novel molecules to inhibit topoisomerase I and II as a means of evaluating their potential antiproliferative and anticancer effects.<sup>60,61</sup>

A series of urea-linked ciprofloxacin-chalcone hybrid compounds were synthesized by ref. 62 and compounds 25 and 26 (Fig. 12), demonstrated remarkable abilities to inhibit cell growth in both colon HCT-116 and leukemia SR cancer cell lines, outperforming the reference compounds camptothecin, topotecan, and staurosporine. Specifically, compounds 25 and 26 exhibited  $IC_{50}$  values of 2.53 and 2.01  $\mu M$ , respectively, against the HCT-116 cell line, and 0.73 and 0.64  $\mu M$ , respectively, against the leukemia SR cell line. These values were significantly lower than those of the reference compounds. In addition to their potent antiproliferative effects, compounds 25 and 26 also showed inhibitory activity against topoisomerase I

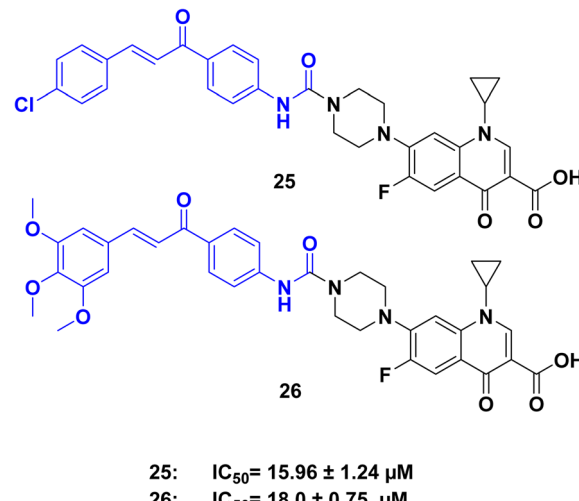


Fig. 12 Ciprofloxacin/chalcone hybrids 25, and 26 as topoisomerase inhibitors.

and II  $\beta$ . Compound 26 exhibited 56.72% inhibition of topoisomerase I and 60.06% inhibition of topoisomerase II  $\beta$ , compared to 60.05% and 71.09% inhibition by the reference compounds camptothecin and topotecan, respectively. Regarding the structure–activity relationship, the study found that replacing three hydrogen atoms on the phenyl ring of the chalcone moiety with methoxy groups resulted in the most active compound. For compounds with a single substituent, a chlorine atom in the *para* position produced the highest activity compared to other halogen or electron-donating groups.

Kim *et al.*<sup>63</sup> conducted a study in which they synthesized a series of chalcone derivatives. The aim of the study was to identify compounds that could inhibit the topoisomerase enzyme and exhibit antiproliferative activity against cancer cells. The synthesized compounds were tested *in vitro* against various cancer cell lines and the topoisomerase enzyme. Compound 27 (Fig. 13), exhibited 100% inhibition of the topoisomerase I enzyme at a concentration of 100  $\mu M$ ,

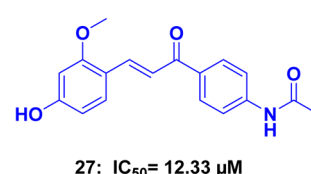
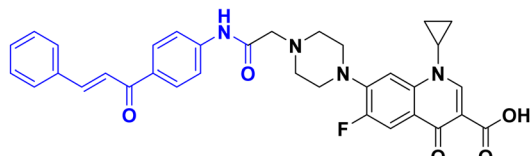
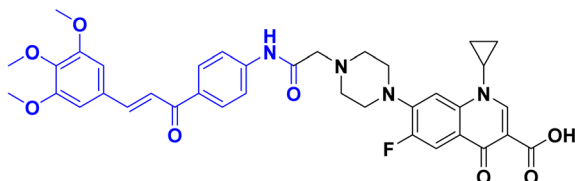


Fig. 13 Chalcone hybrid 27 as topoisomerase inhibitor.





28:  $|C_{50}|$  ranging between 0.42 and 1.87  $\mu M$



29:  $IC_{50}$  = ranging between 0.21 to 57.6  $\mu M$

Fig. 14 Ciprofloxacin/chalcone hybrids **28**, and **29** as Topoisomerase inhibitors

comparable to the positive control camptothecin, which showed 70.5% inhibition at the same concentration. Compound 27 also showed moderate cytotoxic activity against human breast ductal carcinoma cell line (T47D) with an  $IC_{50}$  of 12.33  $\mu$ M and human gastric cancer cell line (SNU638) with an  $IC_{50}$  of 17.41  $\mu$ M.

Abdel-Aziz *et al.*,<sup>64</sup> prepared *N*-4-piperazinyl-ciprofloxacin-chalcone derivatives. The results of a test on a single dose of anticancer compounds showed that compounds **28** and **29** (Fig. 14) were the most effective at inhibiting the growth of various cancer cell lines. In an *in vitro* five-dose test on the full NCI 60 cell panel, compound **28** demonstrated a broad-spectrum antitumor activity against all nine tumor subpanels tested, without significant selectivity. Compound **29**, on the other hand, exhibited high selectivity towards the leukemia subpanel. Most of the tested compounds showed good inhibitory activity against both topoisomerase I and topoisomerase II at 100  $\mu$ M. The study found that the presence of three  $\text{OCH}_3$  groups is more effective than the presence of one  $\text{OCH}_3$  group. Compound **29**, with three  $\text{OCH}_3$  groups, showed superior anti-cancer activity against various cancer cell lines compared to compound **28**, which had one  $\text{OCH}_3$  group. Additionally, the presence of an electron-donating group ( $\text{OCH}_3$ ) in compound **29** was more effective against cancer cells than an electron-withdrawing group.

The studies on chalcone derivatives as topoisomerase I and II inhibitors highlight key structural trends that enhance potency. Methoxy groups, especially in the *para* position, and halogen substitutions, such as chlorine, on the phenyl ring, significantly boost enzyme inhibition. Compounds with three methoxy groups showed stronger antiproliferative effects, suggesting that electron-donating groups improve enzyme inhibition.

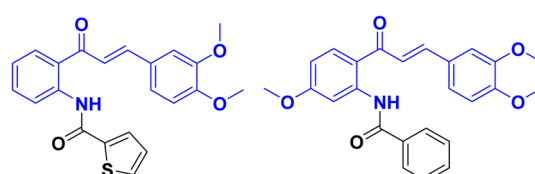
### 3.3 ABCG2 modulators

ABCG2 modulators represent a promising pathway in the development of anticancer drugs. ABCG2, also known as breast

cancer resistance protein (BCRP), is a member of the ATP-binding cassette (ABC) transporter family.<sup>65</sup> It is highly expressed in various tissues, including the intestines, liver, kidney, and blood-brain barrier. The role of ABCG2 in cancer is significant, as it acts as a multidrug efflux pump, pumping out a wide range of chemotherapeutic agents from cancer cells. This efflux activity contributes to drug resistance, limiting the effectiveness of chemotherapy and leading to treatment failure.<sup>66</sup> In recent years, many researches have focused on developing ABCG2 modulators to overcome drug resistance and enhance the efficacy of anticancer drugs.<sup>67</sup> These modulators are compounds that can either inhibit or enhance the activity of ABCG2, thereby influencing its efflux function. Inhibitors of ABCG2 can block the pump's activity, preventing the efflux of anticancer drugs and increasing their intracellular concentration within cancer cells.<sup>68</sup> This approach can sensitize cancer cells to chemotherapy and improve treatment outcomes. On the other hand, enhancers of ABCG2 can stimulate the pump's activity, promoting the efflux of toxic metabolites and protecting normal tissues from drug-induced toxicity.<sup>69</sup>

Kraege *et al.*,<sup>70</sup> synthesized a series of 35 compounds by combining a typical chalcone structure with different acid chlorides. An amide linker was introduced at positions 2', 3', or 4' on ring A of the chalcone. These compounds exhibited a diverse range of substitution patterns, which facilitated the establishment of structure-activity relationships and identification of optimal structural characteristics for further investigation. The inhibitory activity against ABCG2 and intrinsic cytotoxicity of the synthesized acryloylphenylcarboxamides were examined. The study revealed that the *ortho* position of the amide linker and the presence of 3,4-dimethoxy groups on the distal phenyl ring of the chalcone were crucial for inhibitory activity. Additionally, the highest potency was observed with unsubstituted phenyl, thiophene, and quinoline rings linked to the amide group. Compound 30 (Fig. 15), exhibited the most significant activity, with an  $IC_{50}$  of 0.600  $\mu\text{M}$  against MDCK II BCRP cells by using pheophorbide A assay.

Again Kraege *et al.*,<sup>71</sup> synthesized and examined a series of chalcones combined with an additional aromatic residue to evaluate their inhibitory effects on ABC transporters. In their previous mentioned article, they determined that the *ortho* position on the chalcone A-ring was the preferred location for the amide linker, and they discovered various substitution patterns on the additional ring that enhanced potency. In this study, they investigated whether introducing a methoxy group, known to improve the inhibitory activity of chalcones, would



30:  $IC_{50} = 0.6 \mu M$

31:  $IC_{50} = 0.211 \mu M$

Fig. 15 Chalcone hybrids **30**, and **31** as ABCG2 inhibitors.

also be advantageous for the acryloylphenylcarboxamide scaffold. Remarkably, this modification resulted in highly potent ABCG2 inhibitors. To further support the hypothesis regarding the beneficial impact of the amide linker, six acryloylphenylcarboxylates were synthesized and examined for their inhibitory activity. Substituting the amide linker with an ester group led to decreased inhibition. Among the derivatives tested, compound 31 (Fig. 15), exhibited the highest level of activity with  $IC_{50} = 0.211 \mu\text{M}$  against ABCG2. These include the amide linker positioned *ortho*, a 4'-methoxy substitution on ring A, 3,4-dimethoxy groups on ring B, and an unsubstituted phenyl ring connected to the amide linker.

In conclusion, the findings of this study can be summarized as follows: the 3,4-dimethoxy substitution on ring B was found to be beneficial for inhibiting ABCG2, based on previous studies.<sup>72</sup> A 4'-methoxy substitution on ring A of the chalcone moiety was identified as a beneficial structural feature, leading to increased inhibitory activity against ABCG2. However, 4',5'-dimethoxy substitution resulted in slightly decreased potency. There was no significant difference between chalcones substituted with 3,4- or 3,5-dimethoxy groups on ring B, as well as comparable 4'-methoxy-substituted acryloylphenylcarboxamides and benzoates. The replacement of the amide linker with an ester function in the acryloylphenylcarboxylates resulted in decreased inhibitory effects towards ABCG2. This could be attributed to the loss of donor-acceptor behavior or differences in preferred conformation. These findings provide valuable insights into the structure-activity relationships and the potential for developing selective ABCG2 inhibitors. Further studies and optimization of compound design could lead to the development of more potent and selective inhibitors for therapeutic applications.

### 3.4 Caspase protein inhibitors

Caspases are a family of proteins that play a crucial role in the regulation of programmed cell death, known as apoptosis. These proteins act as key players in the intricate network of signaling pathways responsible for maintaining cellular homeostasis.<sup>73</sup> Dysregulation of apoptosis has been implicated in various diseases, including cancer, making caspases attractive targets for the development of anticancer agents.<sup>74</sup> In cancer cells, the dysregulation of apoptotic pathways often leads to uncontrolled cell proliferation and resistance to cell death, contributing to tumor development and progression.<sup>75</sup> Targeting caspases and modulating their activity has emerged as a promising strategy for developing novel anticancer agents.<sup>76</sup> By promoting apoptosis in cancer cells, caspase-targeted therapies aim to induce selective cell death, inhibit tumor growth, and overcome drug resistance.<sup>77</sup> Targeting caspase proteins and their associated apoptotic pathways holds great potential for the development of more effective and selective cancer therapies.<sup>75,78</sup>

Tok *et al.*,<sup>79</sup> synthesized a series of chalcone derivatives and assessed its *in vitro* antiproliferative activities against HeLa, MCF-7, MKN-45 cancer cell lines, as well as the NIH-3T3 cell line using the MTT assay. Notably, compound 32 (Fig. 16), exhibited



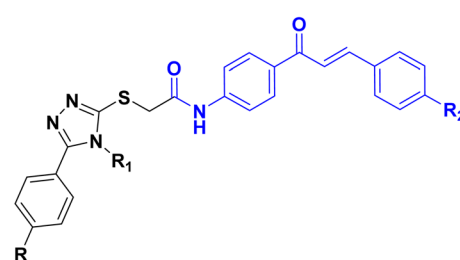
32:  $IC_{50}$  = ranging between 5.17 to 26.6  $\mu\text{M}$

Fig. 16 Chalcone hybrid 32 as caspase inhibitor.

significant cytotoxic effects on all three cancer cells while demonstrating no cytotoxicity towards NIH-3T3 normal cells. The  $IC_{50}$  values for compound 32 were 26.66  $\mu\text{M}$  on HeLa, 9.41  $\mu\text{M}$  on MCF-7, and 5.17  $\mu\text{M}$  on MKN-45. Furthermore, compound 32 exhibited the ability to upregulate the protein expression of Bax while downregulating the protein expression of Bcl-2 in cells. Additionally, these compounds increased caspase-3 activity in the cells. Based on these findings, it can be concluded that 32 activated apoptosis by inducing mitochondrial apoptotic proteins in HeLa, MCF-7, and MKN-45.

Ahmed *et al.*,<sup>80</sup> synthesized a series of hybrids combining 1,2,4-triazole and chalcone. The synthesized compounds demonstrated remarkable cytotoxic activity against various cancer cell lines. Among the tested compounds, compounds 33, 34, 35, 36, 37, and 38 (Fig. 17), exhibited the highest cytotoxicity against human lung adenocarcinoma A549 cells, with  $IC_{50}$  values 19.43, 6.06, 4.4, 7.55, 16.04 and 8.04  $\mu\text{M}$ , respectively. In comparison, cisplatin had an  $IC_{50}$  of 15.3  $\mu\text{M}$ . Further investigation into the mechanism of action revealed that the 1,2,4-triazole-chalcone hybrids induced apoptosis by increasing the level of proapoptotic protein Bax, releasing cytochrome c from mitochondria, and activating caspase-3/8/9 proteins.

In the analysis of the structure-activity relationship (SAR), we found that the presence of *N*-4-allyl triazole in the hybrids resulted in higher activity compared to *N*-4-phenyl triazole. It was observed that for optimal activity in the allyl triazole hybrids, the presence of 3,4,5-trimethoxy groups in  $R_2$  was crucial. Additionally, the chalcone phenyl ring B in these hybrids needed to be substituted with either electron-donating or electron-withdrawing groups (such as  $\text{OCH}_3$  or  $\text{Cl}$ ) preferably



33: R= 4-Cl R <sub>1</sub> = Phenyl R <sub>2</sub> = H	$IC_{50}$ = 19.43 $\mu\text{M}$
34: R= 4-Cl R <sub>1</sub> = Allyl R <sub>2</sub> = 3,4,5-trimethoxy	$IC_{50}$ = 6.06 $\mu\text{M}$
35: R= 4-OCH <sub>3</sub> R <sub>1</sub> = Allyl R <sub>2</sub> = 3,4,5-trimethoxy	$IC_{50}$ = 4.4 $\mu\text{M}$
36: R= 3,4,5-trimethoxy R <sub>1</sub> = Allyl R <sub>2</sub> = 3,4,5-trimethoxy	$IC_{50}$ = 7.55 $\mu\text{M}$
37: R= 3,4-dimethoxy R <sub>1</sub> = Phenyl R <sub>2</sub> = 4-OCH <sub>3</sub>	$IC_{50}$ = 16.04 $\mu\text{M}$
38: R= 3,4,5-trimethoxy R <sub>1</sub> = Phenyl R <sub>2</sub> = 3,4,5-trimethoxy	$IC_{50}$ = 8.04 $\mu\text{M}$

Fig. 17 1,2,4-Triazole/chalcone hybrids 33–38 as caspase inhibitors.



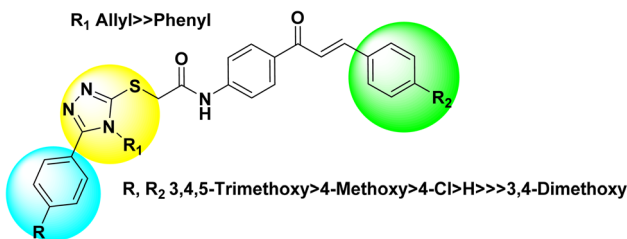


Fig. 18 Structure–activity relationship of the compounds (34–38).

in the *p*-position. However, full substitution of the phenyl ring slightly decreased the activity, while 3,4-dimethoxy substitution greatly reduced it. Nonetheless, the activity was maintained when trimethoxy substitution was present. On the other hand, in the phenyl triazole hybrids, optimal activity was achieved when both R and R<sub>2</sub> were 3,4,5-trimethoxy groups. The activity slightly decreased when the phenyl ring was substituted with electron-donating or electron-withdrawing groups in the *p*-position (Fig. 18).

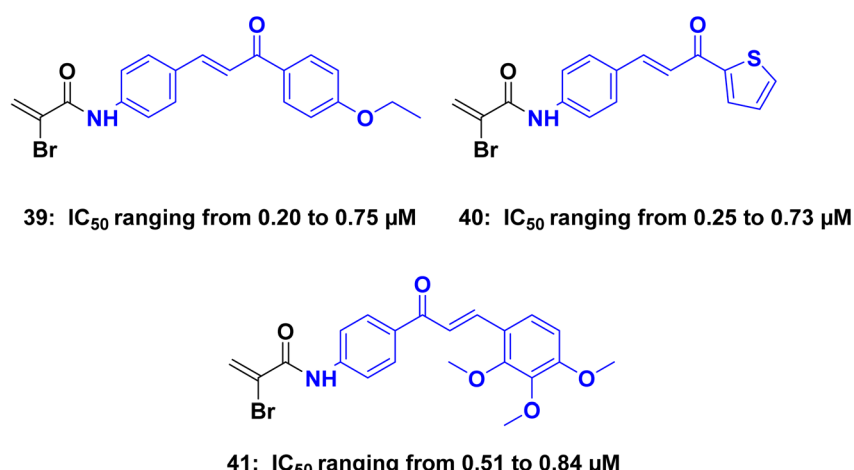
Romagnoli *et al.*<sup>81</sup> synthesized a series of bromoacryloylamido/chalcones hybrids and evaluated for their ability to inhibit the growth of cancer cells in five different cell lines. These hybrid derivatives displayed significantly enhanced anti-tumor activity when compared to the corresponding amino chalcones. The most promising molecules identified as potential leads were compounds **39**, **40**, and **41** (Fig. 19), the anti-proliferative activity of these three compounds was evaluated against five different cancer cell lines: L1210, FM3A, Molt4, CEM, and HeLa. Compound **39** exhibited remarkable activity, with IC<sub>50</sub> values of 0.24  $\mu$ M, 0.68  $\mu$ M, 0.61  $\mu$ M, 0.75  $\mu$ M, and 0.75  $\mu$ M for the respective cell lines. Similarly, compound **40** displayed notable activity, with IC<sub>50</sub> values of 0.25  $\mu$ M, 0.52  $\mu$ M, 0.55  $\mu$ M, 0.73  $\mu$ M, and 0.34  $\mu$ M. Compound **41** also demonstrated significant potency, with IC<sub>50</sub> values of 0.63  $\mu$ M, 0.53  $\mu$ M, 0.68  $\mu$ M, 0.84  $\mu$ M, and 0.51  $\mu$ M. Flow cytometry analysis conducted on K562 cells revealed that the most active compounds caused a substantial proportion of cells to enter the

apoptotic sub-G0–G1 peak, indicating cell death. Compound **39** increased activated caspase-3 after 24 h of treatment, and a further increase after 48 h.

### 3.5 Histone deacetylase (HDAC) inhibitors

Histone deacetylase (HDAC) inhibitors have emerged as promising agents in the development of anticancer therapies. HDACs are enzymes that regulate gene expression by modifying histone proteins, which play a critical role in chromatin remodeling and gene transcription.<sup>82</sup> Dysregulation of HDAC activity is observed in various cancers, promoting tumor growth and progression.<sup>83</sup> HDAC inhibitors target and inhibit these enzymes, leading to the accumulation of acetyl groups on histone proteins. This alters chromatin structure and gene expression, activating tumor suppressor genes and repressing oncogenes.<sup>84</sup> HDAC inhibitors have shown antitumor effects by inducing cell cycle arrest, differentiation, and apoptosis in cancer cells.<sup>85</sup> They have been approved for hematological malignancies and are being investigated for solid tumors.<sup>86</sup>

Valente *et al.*<sup>87</sup> synthesized compounds combining pyrrole and benzene with hydroxamate and chalcone groups. Among the synthesized compounds, **42** and **43** (Fig. 20) exhibited selective inhibition of HDAC6 at the nanomolar level 30 and 10 nM respectively. In human acute myeloid leukemia U937 cells, the other hydroxamates led to increased levels of acetyl- $\alpha$ -tubulin. Furthermore, in the same U937 cell line, compounds **42** and **43** demonstrated apoptotic effects of 18.4% and 21.4%, respectively, compared to 16.9% for SAHA (a reference HDAC inhibitor). The antiproliferative effects of compound **43** were also investigated across various cancer cell lines. It showed growth inhibition at sub-micromolar concentrations in neuroblastoma LAN-5 and SH-SY5Y cells, as well as chronic myeloid leukemia K562 cells. Moreover, in lung H1299 and A549, colon HCT116 and HT29 cancer cells, compound **43** exhibited growth inhibition at low-micromolar concentrations. In HT29 cells, compound **43** increased histone H3 acetylation and significantly reduced the colony forming potential of the cancer cells by up to 60%.

Fig. 19 Chalcone hybrids **39–41** as caspase inhibitors.

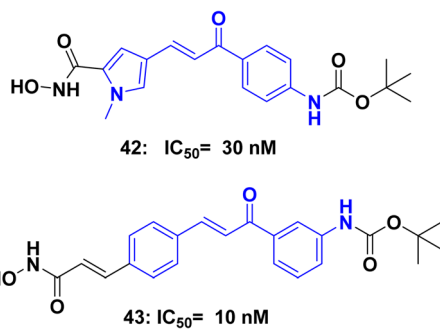


Fig. 20 Chalcone/hydroxymate hybrids 42, and 43 as HDAC inhibitors.

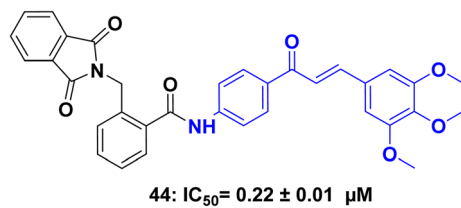


Fig. 21 Chalcone hybrid 44 as HDAC inhibitor.

A series of chalcone-based hybrids with  $\alpha$ -phthalimido substituents as a dual inhibitors targeting histone deacetylases (HDACs) and tubulin for potential anticancer applications.<sup>88</sup> The synthesized compounds were evaluated for their anticancer activity against MCF-7 and HepG2 human cancer cell lines using the MTT assay. They measured the *in vitro*  $\beta$ -tubulin polymerization and inhibitory activity against HDAC 1 and 2 for the most potent hybrids. Among the compounds tested, the trimethoxy derivative 44 (Fig. 21) exhibited the highest anticancer activity. It demonstrated potent  $\beta$ -tubulin polymerase and HDAC 1 and 2 inhibitory activity with  $IC_{50}$  of  $0.22 \pm 0.01 \mu\text{M}$  against HDAC 1. Additionally, compound 44 effectively induced cell cycle arrest at both the G2/M and preG1 phases in the MCF-7 cell line.

### 3.6 Tubulin polymerization inhibitors

Tubulin polymerization inhibitors are a class of compounds that play a crucial role in the field of medicinal chemistry. These inhibitors target the process of microtubule assembly and disassembly,<sup>89</sup> which is essential for cellular functions such as cell division, intracellular transport, and maintenance of cell shape. By interfering with tubulin polymerization, these inhibitors disrupt the formation of microtubules, leading to cell cycle arrest and inhibition of cell proliferation.<sup>90</sup> They have shown significant promise as anticancer agents, as they selectively target rapidly dividing cancer cells. Tubulin polymerization inhibitors exhibit various mechanisms of action, including binding to tubulin subunits, preventing their assembly into microtubules, or destabilizing existing microtubule structures. This disruption of microtubule dynamics ultimately leads to cell death through apoptosis or mitotic catastrophe.<sup>91</sup> Ongoing research aims to discover and optimize novel tubulin polymerization inhibitors with improved efficacy, selectivity, and

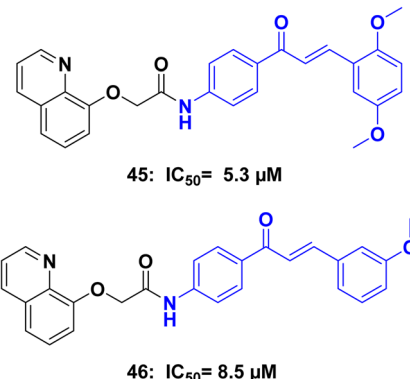


Fig. 22 Chalcone/quinoline hybrids 45, and 46 as tubulin inhibitors.

reduced toxicity, paving the way for the development of more effective treatments against cancer and other diseases characterized by uncontrolled cell growth.<sup>92</sup>

Amin *et al.*<sup>93</sup> Synthesized a series of 8-hydroxyquinoline/chalcone hybrids, and investigated for their potential anticancer activity. Notably, compounds 45 and 46 (Fig. 22) demonstrated exceptional activity against both HCT116 and MCF7 cells, while also showing improved safety towards normal WI-38 cells when compared to staurosporine. Further enzymatic assays indicated that compounds 45 and 46, displayed effective inhibition of tubulin polymerization, with  $IC_{50}$  values of 5.3 and 8.5  $\mu\text{M}$  respectively, in comparison to the reference compound combretastatin A4 ( $IC_{50} = 2.15 \mu\text{M}$ ). Additionally, compounds 45, and 46 demonstrated inhibition of EGFR (epidermal growth factor receptor), with  $IC_{50}$  values of 0.097  $\mu\text{M}$ , and 0.334  $\mu\text{M}$ , respectively, in contrast to erlotinib ( $IC_{50} = 0.056 \mu\text{M}$ ). Compounds 45 and 46 were further investigated to assess their effects on the cell cycle, induction of apoptosis, and suppression of the wnt1/ $\beta$ -catenin gene. Western blot analysis was conducted to detect the apoptosis markers Bax, Bcl2, Casp3, Casp9, PARP1, and  $\beta$ -actin.

A series of chalcone derivatives synthesized and their anti-proliferative activities were assessed against five human tumor cells.<sup>94</sup> These chalcone derivatives contain an additional aromatic or heterocyclic ring connected *via* an ether or an ester or an amide functional group. Furthermore, the impact of the presence of one or three methoxy groups or a 2,4-dimethoxy-3-methyl system on the B ring of the chalcone structure on cytotoxicity was investigated. The findings demonstrated that the most cytotoxic chalcones contained a furoyl substituent connected through an ester or an amide to the 2'-hydroxy or 2'-amino group of the A ring in the chalcone skeleton. These compounds exhibited  $IC_{50}$  values ranging from 0.2  $\mu\text{M}$  to 1.3  $\mu\text{M}$  against human leukemia cells. Specifically, the synthetic compound 47 (Fig. 23) exhibited at least ten-fold greater potency than the antineoplastic agent etoposide against U-937 cells, while showing lower cytotoxicity against human peripheral blood mononuclear cells. Treatment of U-937 and HL-60 cells with FMC resulted in cell cycle arrest at the G2-M phase, an increase in the percentage of sub-G1 and annexin-V positive cells, release of mitochondrial cytochrome c, activation of caspase, and cleavage of poly(ADP-ribose) polymerase.

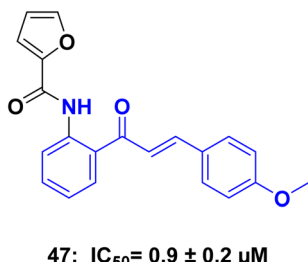


Fig. 23 Chalcone hybrid 47 as tubulin inhibitor.

### 3.7 Miscellaneous anticancer chalcone acetamides

Histone lysine specific demethylase 1 (LSD1) has gained significant attention as a promising molecular target for the development of potent anticancer drugs to combat leukemia. Li, Y., *et al.*<sup>95</sup> synthesized a series of chalcone derivatives and assessed their inhibitory activity against LSD1. All chalcone-dithiocarbamate hybrids demonstrated considerable inhibitory activity against LSD1. Notably, chalcone **48** (Fig. 24), exhibited the most potent LSD1 inhibitory activity, with an  $IC_{50}$  value of  $0.14 \mu M$ . Furthermore, compound **48** displayed inhibitory effects on cell proliferation, with  $IC_{50}$  values of  $1.10 \mu M$ ,  $3.64 \mu M$ ,  $3.85 \mu M$ ,  $1.87 \mu M$ ,  $0.87 \mu M$ , and  $2.73 \mu M$  against HAL-01, KE-37, P30-OHK, SUP-B15, MOLT-4, and LC4-1 leukemia cells, respectively. Additional investigations revealed that compound **48** selectively and reversibly inhibited LSD1 in a time-dependent manner. It also up-regulated the expression levels of H3K9me1 and H3K9me2 in MOLT-4 cells. Notably, in an *in vivo* xenograft model, chalcone **48** inhibited tumor growth without causing apparent toxicity.

A series of chalcone-dithiocarbamate hybrids and assessed their ability to inhibit cell proliferation in various cancer cell lines, including MGC803, MCF7, and PC3.<sup>96</sup> Among these hybrids, compound **49** (Fig. 24), exhibited the most potent inhibitory activity against PC3 cells, with an  $IC_{50}$  value of  $1.05 \mu M$ . Preliminary investigations into the biological mechanisms of compound **49** revealed several effects. It was found that **49** could reduce colony formation, induce DNA damage, and arrest the cell cycle at the G2/M phase. This effect was associated with the upregulation of P21 and the downregulation of CDK1 and cyclinB1, and it occurred in a concentration-dependent manner. Notably, **49** also induced apoptosis in PC3 cells by reducing the mitochondrial membrane potential and altering the expression levels of BCL-2 family proteins. Additionally, as an apoptosis inducer, **49** triggered the accumulation of intracellular reactive oxygen species (ROS) in PC3 cells by inhibiting the activity of the catalase enzyme.

Lamie & Philloppe,<sup>97</sup> synthesized a group of hybrid compounds combining 2-thiopyrimidine and chalcone, and its cytotoxic activities were assessed against three different cell lines: K-562, MCF-7, and HT-29. Most derivatives exhibited significant activity against the K-562 cell line, with  $IC_{50}$  values ranging from  $0.77$  to  $1.74 \mu M$ . Against the MCF-7 cell line, the  $IC_{50}$  values ranged from  $1.37$  to  $3.56 \mu M$ , while against the HT-

29 cell line, the  $IC_{50}$  values ranged from  $2.10$  to  $2.37 \mu M$ . Furthermore, five derivatives were selected for further evaluation of their cytotoxicity against the normal fibroblast cell line WI38. Additionally, the inhibitory activities against STAT3 and STAT5a were determined for the most active derivatives. Notably, compound **50** (Fig. 24), exhibited dual inhibitory activity, with  $IC_{50}$  values of  $113.31$  and  $50.75 \mu M$  against STAT3 and STAT5a, respectively.

Ren *et al.*<sup>98</sup> synthesized homoserine lactones/chalcone hybrids. These compounds were then tested *in vitro* to evaluate their cytotoxic activity against four different human cancer cell lines. Compounds with the chalcone scaffold exhibited significantly increased cytotoxicity compared to compounds with hydrophobic side chains. Additionally, certain compounds showed higher potency than the commonly used drug 5-Fu and a natural compound called OdDHL. Among the compounds tested, those with the 4-amino chalcone scaffold demonstrated excellent inhibition against all cancer cell lines, surpassing the effectiveness of 5-Fu. Compound **51** (Fig. 24), which contained a 3,4,5-trimethoxy group with  $IC_{50}$   $1.32 \mu M$ , proved to be the most potent against all cancer cell lines. Further analysis using flow cytometry revealed that analog **52** with  $IC_{50}$  of  $5.57 \mu M$  induced cellular apoptosis and cell cycle arrest at the G2/M phase of MCF-7 cells in a concentration- and time-dependent manner.

M. A. Mourad,<sup>99</sup> synthesized a group of nitric oxide (NO) releasing chalcones by combining amino chalcones with different NO-releasing moieties such as nitrate esters, oximes, and furoxans. The compounds were then screened to evaluate their potential as anticancer agents, and the results demonstrated a range of cytotoxic activity, varying from mild to strong. Among the NO-releasing compounds tested, compounds **53** and **54** (Fig. 24), displayed notable cytotoxic activity against a diverse set of cancer cell lines, including leukemia, lung, renal, breast, colon, melanoma, ovarian, and skin cancer cells. The nitrate ester compound **53** exhibited the highest level of inhibitory activity. Additionally, compound **53** exhibited moderate selectivity specifically towards colon cancer, with a selectivity ratio of  $5.87$  at the TGI (total growth inhibition) level.

Cao *et al.*<sup>100</sup> designed and synthesized Pt(iv) complexes that were combined with P-glycoprotein (P-gp) inhibitors to overcome resistance (MDR) and improve the effectiveness of anti-cancer treatments. Among these complexes, complex **55** (Fig. 24), demonstrated notable abilities: it efficiently reversed cisplatin resistance in the SGC-7901/CDDP cell line, with an  $IC_{50}$  value of  $3.37 \mu M$ , and exhibited an increased selectivity index of  $6.9$  against the normal HL-7702 cell line. Detailed investigations conducted on SGC-7901/CDDP cells provided insights into the mechanisms behind the efficacy of complex **55**. It was found that the complex induced apoptosis effectively by suppressing the expression of P-gp, leading to improved cellular uptake of platinum. Moreover, it arrested cells at the G2/M phase, induced DNA damage, and initiated the mitochondrial apoptosis pathway. Furthermore, *in vivo* studies demonstrated that the enhanced accumulation of complex **55** resulted in a tumor inhibition rate of  $75.6\%$  in SGC-7901/CDDP xenografts, surpassing the rates achieved by cisplatin ( $25.9\%$ )



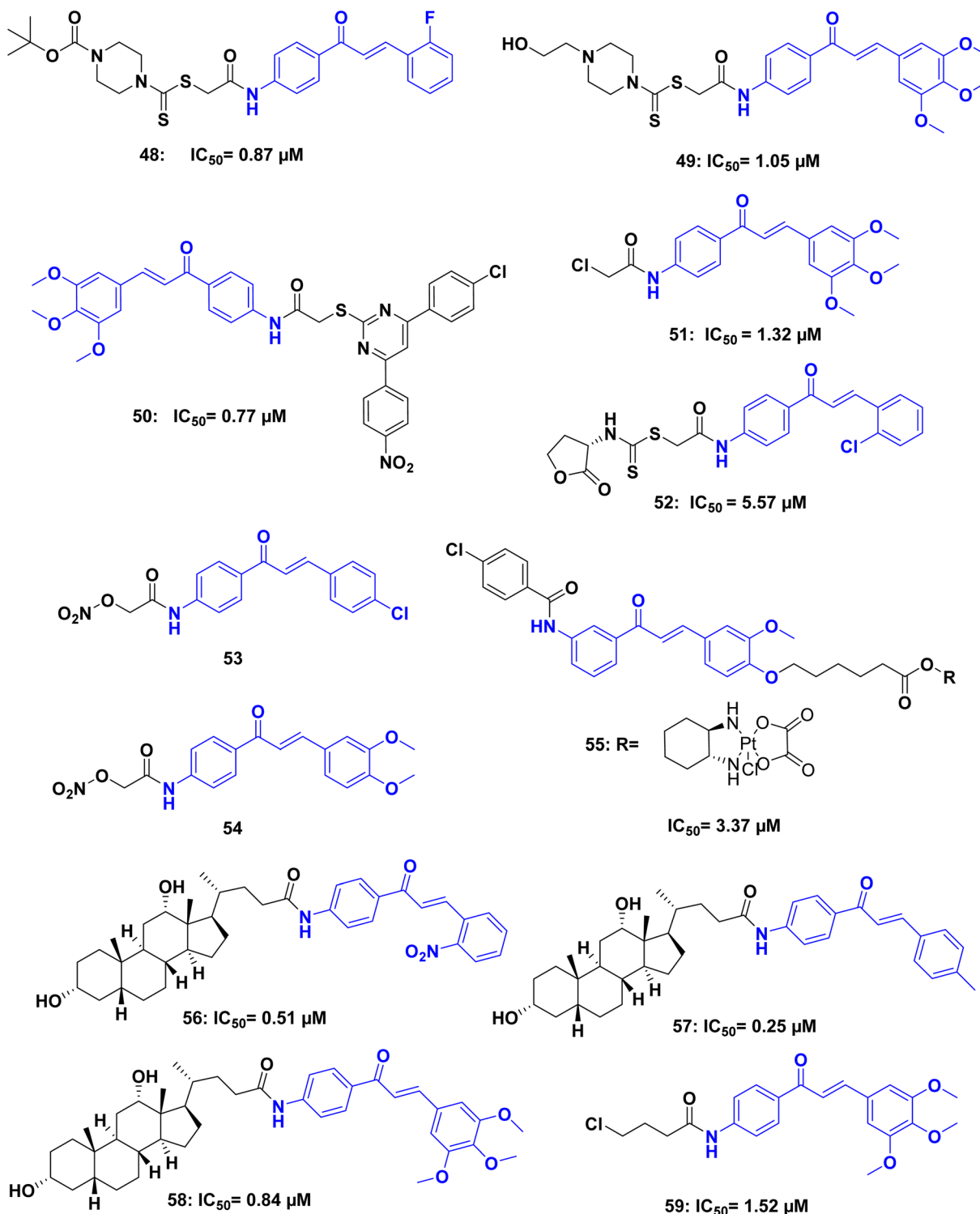


Fig. 24 Miscellaneous anticancer chalcone hybrids 48–59.

and oxaliplatin (43%). Additionally, the low systemic toxicity of complex 55 indicated its potential as a P-gp-mediated MDR modulator.

Patel *et al.*<sup>101</sup> synthesized a series of amides combining deoxycholic acid and chalcone synthesized and evaluated

against two cancer cell lines: A549 (human lung cancer) and SiHa (cervical cancer). Among the synthesized deoxycholic acid–chalcone conjugates, several compounds exhibited promising anticancer activity *in vitro*. Specifically, conjugates 56 ( $IC_{50}$ : 0.51  $\mu\text{M}$ ) and 58 ( $IC_{50}$ : 0.84  $\mu\text{M}$ ) (Fig. 24), containing 2-nitrophenyl

and 3,4,5-trimethoxyphenyl groups respectively, demonstrated good activity against the SiHa cell line. Similarly, compounds **57** ( $IC_{50}$ : 0.25  $\mu$ M) and **56** ( $IC_{50}$ : 1.71  $\mu$ M) showed improved activity against the A549 lung cancer cell line compared to deoxycholic acid and chalcones alone. The conjugation of chalcones with deoxycholic acid resulted in enhanced anticancer activity compared to the individual components. This suggests that employing a bile acid conjugate strategy could be advantageous in enhancing the biological effectiveness of chalcone derivatives. The increased activity observed in certain compounds might be attributed to their improved bioavailability.

Lu *et al.*<sup>102</sup> synthesized Amino chalcone derivatives and investigated for their antiproliferative activity *in vitro*. Several

compounds exhibited moderate to good activity against three human cancer cell lines: MGC-803, HCT-116, and MCF-7 cells. Notably, compound **59** (Fig. 24), displayed the most potent antiproliferative activity, with  $IC_{50}$  values of 1.52  $\mu$ M (MGC-803), 1.83  $\mu$ M (HCT-116), and 2.54  $\mu$ M (MCF-7), surpassing the efficacy of the positive control (5-Fu). Further investigations were conducted to understand the mechanisms involved. The colony formation assay indicated that compound **59** inhibited the formation of cell colonies in MGC-803 cells. DAPI fluorescent staining and flow cytometry analysis revealed that compound **59** induced apoptosis in MGC-803 cells. Additionally, western blotting experiments demonstrated that compound **13e** triggered cell apoptosis through the extrinsic/intrinsic apoptosis

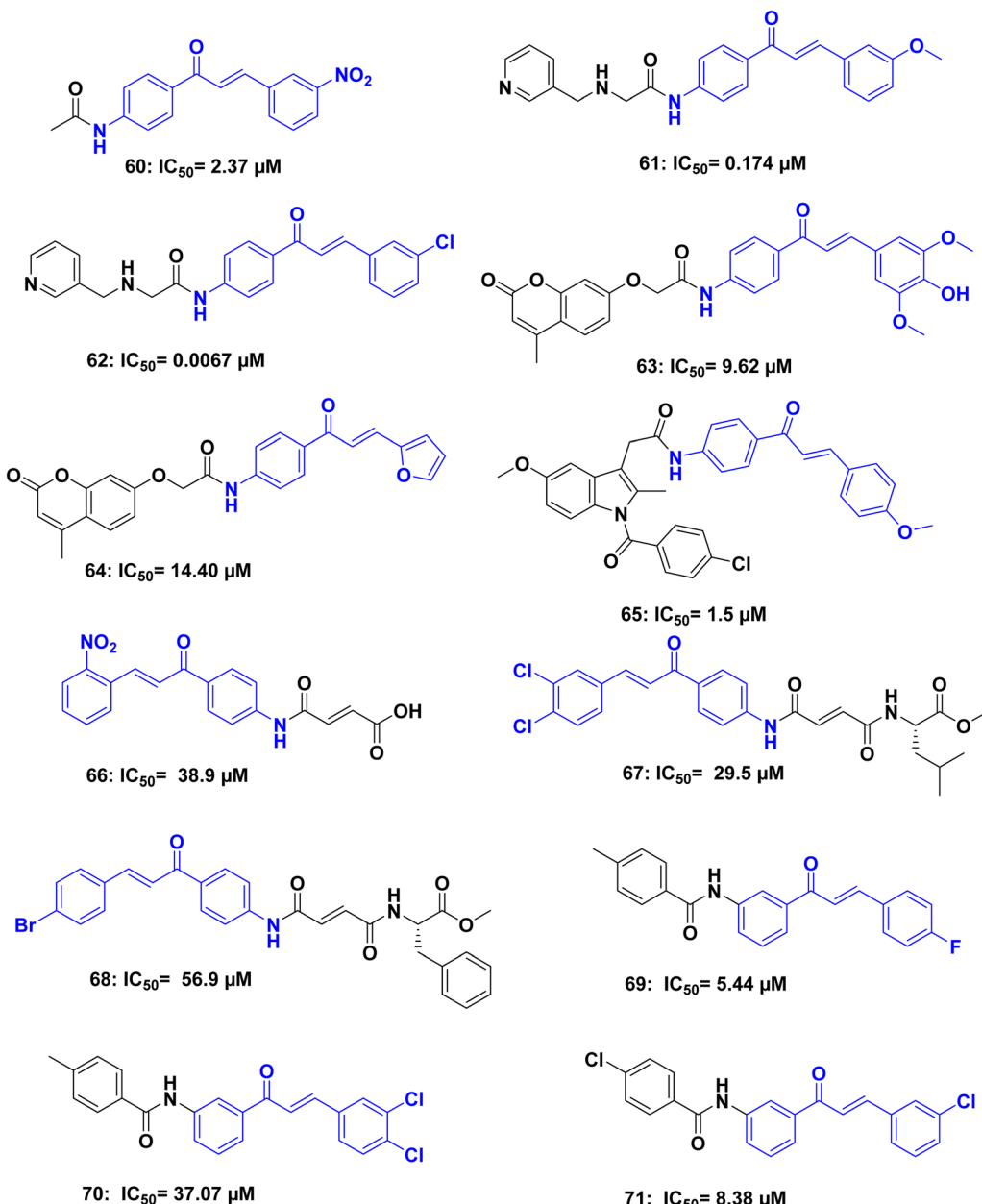


Fig. 25 Chalcone hybrids **60**–**71** with different targets.



pathway in MGC-803 cells. These findings suggest that compound **59** holds promise as a valuable lead compound for antiproliferative agents, and further efforts should be made to enhance the potency of amino chalcone derivatives.

P. N. Bandeira *et al.*<sup>103</sup> synthesized a series of acetamido-chalcone derivatives and subjected to initial biological screening using HCT-116 cells. Among the compounds tested, chalcone **60** (Fig. 25), exhibited potent and specific activity against HCT-116 cells, with an  $IC_{50}$  value of  $2.37 \pm 0.73 \mu\text{M}$ . Preliminary analysis of the structure–activity relationship suggested that the cytotoxic effects of these compounds might be attributed to the combined action of two electron-withdrawing groups: the nitro group ( $\text{NO}_2$ ) located at the *meta*-position of ring B and the acetyl group positioned at the *para*-position of ring A. Furthermore, chalcone **60** demonstrated the ability to induce G2/M cell cycle arrest and apoptosis when incubated at a concentration of  $10 \mu\text{M}$  for 24 hours.

Durgapal *et al.*<sup>104</sup> synthesized a series of chalcone derivatives containing 3-aminomethyl pyridine synthesized and evaluated for their anticancer activity and DNA binding affinity *in vitro*. Most of the compounds exhibited significant antimitotic activity against the A549 cell line, surpassing the effectiveness of fluorouracil. Compounds **61** and **62** (Fig. 25), were specifically chosen for DNA-binding studies due to their excellent activity against cancer cell lines in the MTT assay. The binding affinity of compounds **61** and **62** to CT-DNA was investigated using UV-based DNA titration and fluorescence emission studies in the presence of DNA–EtBr complex. Notably, compound **62** demonstrated remarkable antiproliferative activity, with an  $IC_{50}$  value of  $0.0067 \pm 0.0002 \mu\text{M}$ , against the MCF-7 cell line. Cytotoxicity studies using MTT, LDH, as well as EtBr/AO assay revealed that compound **62** induced apoptosis in the cancerous cell line.

El-Sherief *et al.*<sup>105</sup> constructed a study with an objective to explore a synthesis approach utilizing a molecular hybridization strategy by incorporating a nitric oxide-releasing moiety, oxime, into coumarin-chalcone hybrids. Multiple derivatives were synthesized, and their *in vitro* anti-proliferative activity was evaluated. Moderate activity was observed for some of the prepared compounds, with growth inhibition values of 40.86, and 39.25 for compound against leukemia, central nervous system, and breast cancer cells, respectively. Additionally, compounds **63** and **64** (Fig. 25), exhibited  $IC_{50}$  values of 9.62 and 14.40, respectively, against breast Michigan Cancer Foundation-7 cell lines.

Farrag *et al.*<sup>106</sup> synthesized a series of indomethacin analogs with the aim of investigating their effects on three human colon cancer cell lines: HCT-116, HT-29, and Caco-2. The MTT assay was employed to assess the cytotoxicity of these derivatives. The results from the cytotoxicity assay revealed that the indomethacin amide analog **65** (Fig. 25), displayed remarkable antitumor activity specifically against Caco-2 cells, with an  $IC_{50}$  value of  $1.5 \mu\text{M}$ .

Rodrigues *et al.*<sup>107</sup> synthesized a series of chalcone derivatives hybridized with 4-maleamic acid and 4-maleamide peptidyl groups and evaluated *in vivo* and *in vitro* for their antitumor activity against human prostate cancer. A total of twenty-one compounds were tested, and three of them **66**, **67**, and **68** (Fig. 25), exhibited activities against both androgen-independent (PC-3) and androgen-sensitive (LNCaP) human

prostate cancer cells. Of particular interest was compound **67**, an analog of 4-maleamide peptidyl chalcone, which incorporated a leucine amino acid as a substituent group. This compound demonstrated the highest cytotoxicity among the tested compounds in both tumor cell lines, with an  $IC_{50}$  value of  $29.5 \mu\text{g mL}^{-1}$  for PC-3 cells and  $21.4 \mu\text{g mL}^{-1}$  for LNCaP cells.

Bhojwani *et al.*<sup>108</sup> synthesized chalcone/benzamide hybrids, aiming to investigate their effectiveness as inhibitors of c-Met kinase. Chalcone analogs containing 4-methylbenzamide and 4-chlorobenzamide were synthesized, characterized, and subsequently assessed for their antiproliferative activity using the sulforhodamine-B stain (SRB) assay on various cell lines, including Michigan Cancer Foundation-7 (MCF-7), HT-29, MDA-MB-231, COLO-205, and A549. Compound **70** and compound **71** (Fig. 25), showed  $GI_{50}$  15.6, 6.05  $\mu\text{M}$  respectively which demonstrated better activity than sorafenib ( $GI_{50} = 10.79 \mu\text{M}$ ) in the breast cancer cell line MCF-7, indicating their potential as anticancer agents for breast cancer treatment. Furthermore, all tested compounds, including **69**, **70**, and **71** exhibited excellent activity in the colon cancer cell line, suggesting their effectiveness in colon cancer treatment. In the lung cancer cell line, compound **69** showed better activity than sorafenib, making it a potential candidate for lung cancer treatment. These promising results highlight the potential of these compounds as anticancer agents.

Lakshmanan *et al.*<sup>109</sup> synthesized a series of paracetamol chalcone derivatives and evaluated for their cytotoxic activity. The synthesized compounds **72**, **73**, and **74** (Fig. 26), have been examined and it is confirmed that the most promising cytotoxicity and also cell morphology analysis exhibited good apoptotic activity against lung cancer A549 cell.

Um, Y., *et al.*<sup>110</sup> synthesized unsymmetrical curcuminoids with various amide groups and evaluated for their ability to reverse multidrug resistance (MDR). The MDR reversal activity was assessed using the potent anticancer agents, vincristine and paclitaxel, against P-gp non-expressing KB cells and P-gp expressing KBV20C cells. Verapamil was used as a positive control for comparison. Among the compounds tested, **75**, **76**, and **77** (Fig. 26), exhibited potent MDR reversal activity by inhibiting the drug efflux function of P-gp. The remaining compounds showed moderate potency. Based on the preliminary structure–activity relationship analysis, it was observed that the curcumin half-structure, feruloyl benzamidobenzene, holds promise as a lead structure for developing MDR reversal agents. Furthermore, the presence of one or two chloride groups at the *meta*- or *para*-position on benzamide was found to enhance the MDR reversal activity.

A set of chalcone/sulfonylurea hybrids was synthesized by Avupati, V. R.,<sup>111</sup> and compounds were subjected to *in vitro* testing to assess their cytotoxicity and antimicrobial activities. In terms of cytotoxicity, compounds **78** and **79** (Fig. 26), demonstrated significant activity in the brine shrimp lethality assay, with  $ED_{50}$  values of  $3.96 \pm 0.21$  and  $4.02 \pm 0.19 \text{ lg mL}^{-1}$ , respectively. These values were comparable to the reference drug podophyllotoxin, which had an  $ED_{50}$  value of  $3.61 \pm 0.17 \text{ lg mL}^{-1}$ . The findings suggest that compounds **78** and **79** hold potential as starting points for the development of lead molecules with strong cytotoxic effects.



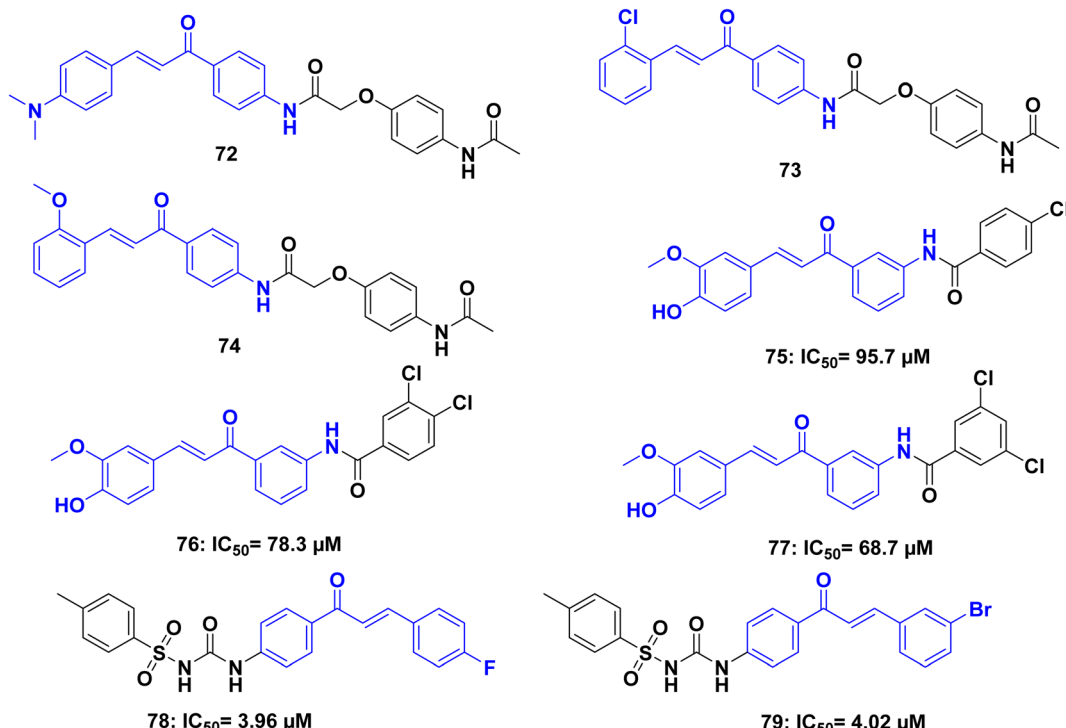


Fig. 26 Anticancer chalcone acetamide hybrids 72–79 with different targets.

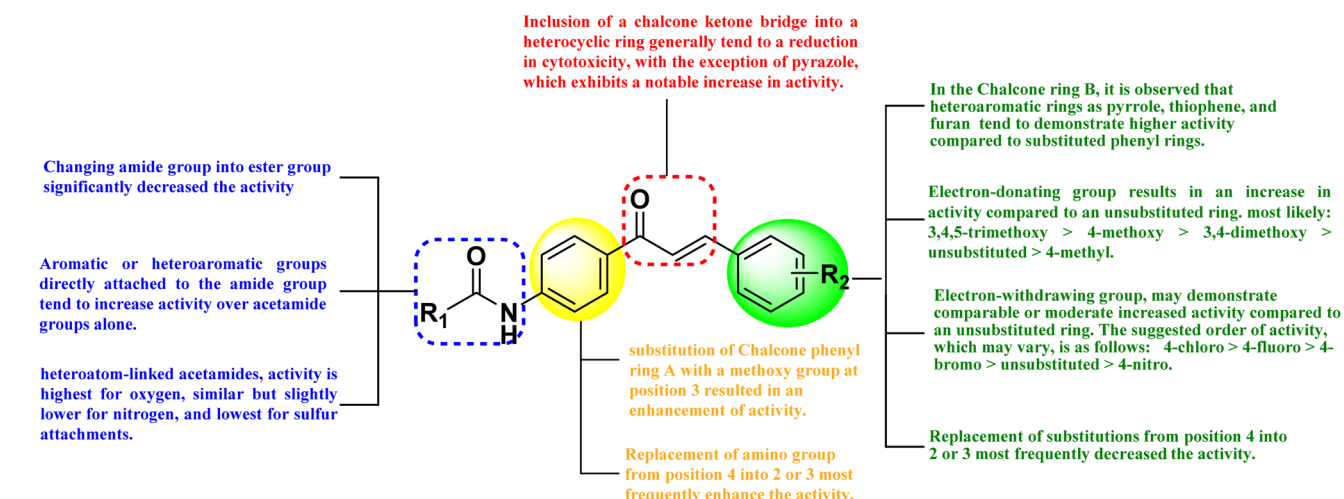


Fig. 27 Suggested structure–activity relationship of amide linked chalcone as anticancer.

### 3.8 Structure–activity relationship of chalcone amide as anticancer

To conclude the SAR analysis, systematic examination of the structural features of the most potent and promising anticancer chalcone derivatives identified in the reviewed literature were obtained. Statistical evaluation was performed on key structural components, including the chalcone phenyl rings A and B, the chalcone ketone bridge, and the amide group attached to the chalcone moiety. By analyzing the relationship between these structural features and the anticancer activity, the most

influential modifications that enhance potency were identified. The introduction of an electron-donating group to the phenyl ring, in certain instances, results in an increase in activity compared to an unsubstituted ring, most likely: 3,4,5-trimethoxy > 4-methoxy > 3,4-dimethoxy > unsubstituted > 4-methyl. The substitution of a phenyl ring with an electron-withdrawing group, in certain cases, may result in comparable activity (in the case of fluorine isostere to hydrogen) or a moderate increase in activity compared to an unsubstituted ring. The suggested order of activity, which is subject to variation, is as follows: 4-chloro > 4-fluoro > 4-bromo > unsubstituted > 4-nitro. However, it is

important to note that these observations are speculative and may not hold true universally (Fig. 27).

## 4 Antimicrobial properties

Antimicrobial resistance has become a global health concern, necessitating the development of effective antimicrobial agents.<sup>112</sup> Chalcones offer promising opportunities in this context, as they have exhibited antimicrobial activity against a broad spectrum of pathogens, including bacteria, and fungi.<sup>113</sup> Multiple mechanisms have been proposed to explain their antimicrobial action, such as inhibiting essential enzymes, disrupting microbial membranes, and interfering with cellular signaling pathways.<sup>114</sup> The antimicrobial potential of chalcones has been evaluated against various drug-resistant strains, including methicillin-resistant *Staphylococcus aureus* (MRSA) and multidrug-resistant *Escherichia coli* (MDR *E. coli*).<sup>115</sup> Additionally, chalcones have demonstrated antifungal activity

against clinically relevant fungi, such as *Candida* species.<sup>116</sup> Furthermore, the structural versatility of chalcones allows for the synthesis of numerous analogs with modified functional groups, leading to enhanced antimicrobial activity and selectivity.<sup>117</sup>

H. H. Mohammed *et al.*,<sup>118</sup> synthesized a series of hybrids combining ciprofloxacin with chalcones, linked by urea group. The antibacterial activity of these compounds was evaluated against *S. aureus*, *P. aeruginosa*, *E. coli*, and *C. albicans* strains. The ciprofloxacin derivatives **2a–j** exhibited broad-spectrum antibacterial activity, with MIC values ranging from 0.06 to 42.23  $\mu\text{g mL}^{-1}$ , compared to ciprofloxacin alone, which had an MIC range of 0.15 to 3.25  $\mu\text{g mL}^{-1}$ . Notably, hybrids **80**, and **81** (Fig. 28), demonstrated significant antibacterial activity, with MIC values ranging from 0.06 to 1.03  $\mu\text{g mL}^{-1}$  against the tested bacterial strains. Moreover, compounds **82**, **81**, exhibited antifungal activity against *Candida albicans* comparable to that of ketoconazole, with MIC values 2.03 to 3.89  $\mu\text{g mL}^{-1}$  respectively.

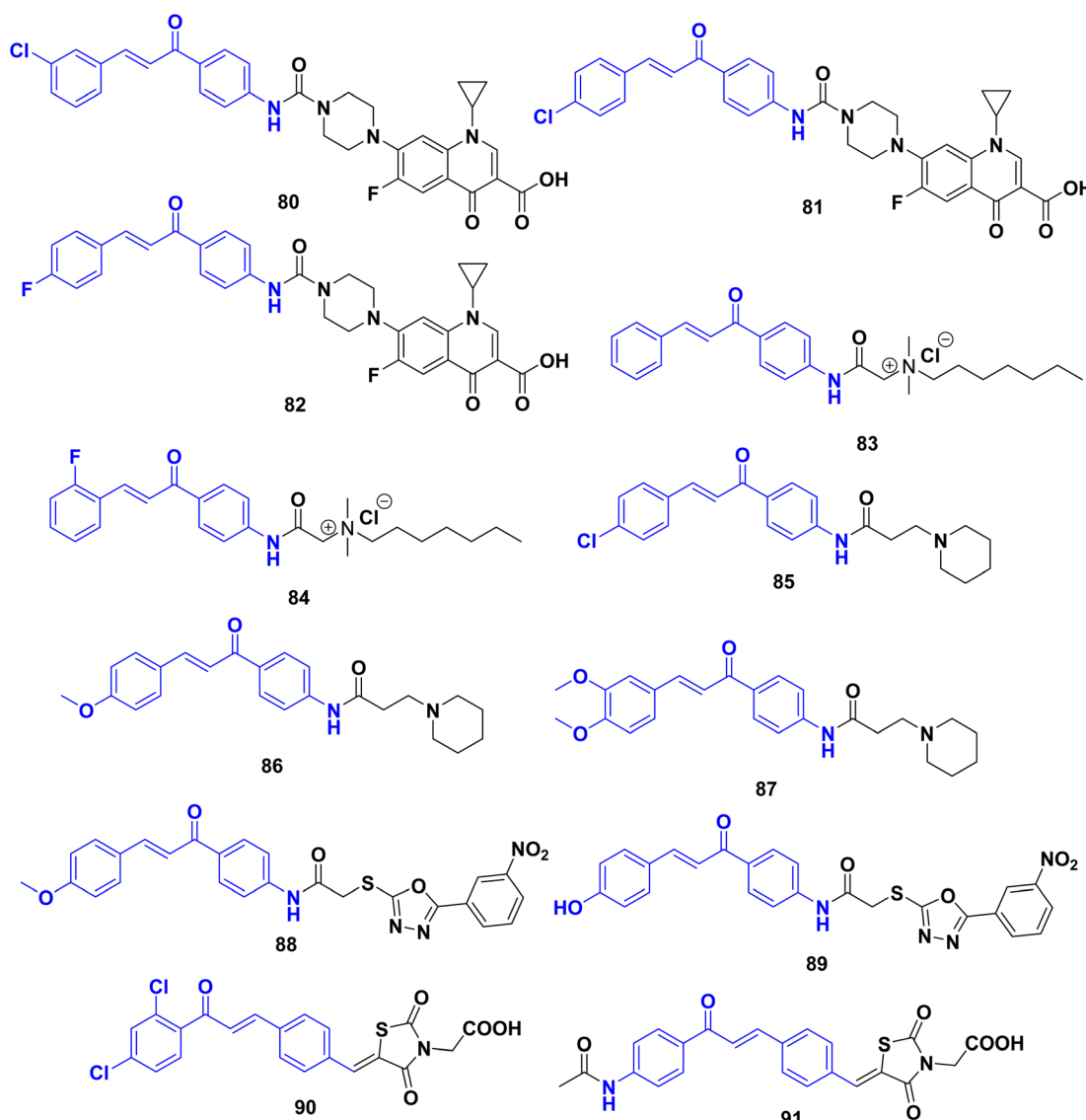


Fig. 28 Chalcone acetamides **80–91** with antibacterial activity.



Further investigations revealed that some of the ciprofloxacin hybrids showed inhibitory activity against DNA gyrase, a potential molecular target, with  $IC_{50}$  values ranging from  $0.231 \pm 0.01$  to  $7.592 \pm 0.40$   $\mu\text{M}$ , compared to ciprofloxacin with an  $IC_{50}$  value of  $0.323 \pm 0.02$   $\mu\text{M}$ .

W.-C. Chu *et al.*<sup>119</sup> synthesized a set of chalcone derivatives to mimic the characteristics of cationic antimicrobial peptides. The antibacterial activities of these compounds were assessed against various drug-sensitive bacteria, including *Staphylococcus aureus*, *Enterococcus faecalis*, *Escherichia coli*, and *Salmonella enterica*. Additionally, clinical isolates of methicillin-resistant *S. aureus* (MRSA), as well as carbapenem-resistant Enterobacteriaceae producing KPC-2 and NDM-1, were evaluated. Among the compounds tested, representative molecules **83** and **84** (Fig. 28), demonstrated potent bactericidal activity against both Gram-positive and Gram-negative bacteria, including drug-resistant strains such as MRSA, KPC, and NDM. Compound **83** exhibited a minimum inhibitory concentration (MIC) of  $1 \text{ mg mL}^{-1}$  against *S. aureus* and  $0.5 \text{ mg mL}^{-1}$  against MRSA, while compound **83** showed an MIC of  $0.5 \text{ }\mu\text{g mL}^{-1}$  against *S. aureus* and  $0.25 \text{ }\mu\text{g mL}^{-1}$  against MRSA. These membrane-active antibacterial compounds effectively reduced the viable cell counts in bacterial biofilms and did not promote the development of bacterial resistance. Furthermore, these representative molecules exhibited minimal toxicity to mammalian cells at appropriate concentrations.

Another series of chalcones containing amide groups and conjugated with various secondary amines were synthesized and assessed for their antibacterial *in vitro* activity.<sup>120</sup> Among the series of compounds, **85**, **86**, and **87** (Fig. 28), exhibited notable activity against different bacterial strains, with MIC values ranging from  $2.0$  to  $10.0 \text{ }\mu\text{g mL}^{-1}$ . Compound **85** showed comparable potency to the standard drug Ampicillin, with an MBC value of  $2.0 \text{ }\mu\text{g mL}^{-1}$  against the bacterial strain *Staphylococcus aureus*. Furthermore, the compounds were evaluated for their anti-biofilm activity. Compounds **85**, **86**, and **87** demonstrated promising anti-biofilm effects, with  $IC_{50}$  values ranging from  $2.4$  to  $8.6 \text{ }\mu\text{g}$ . Molecular modeling studies were conducted to explore the potential anti-biofilm mechanisms. The results suggested that the AspB327 and HisB340 residues, involved in arene–arene interactions, played a crucial role in inhibiting c-di-GMP. Additionally, the hydrophobic nature of the compounds seemed to be important for their activity. ADME calculations were performed, indicating that compounds **85**, **86**, and **87** have the potential to be orally absorbed as effective anti-biofilm agents.

Joshi *et al.*<sup>121</sup> synthesized a series of chalcones containing 1,3,4-oxadiazole derivatives as antimicrobial agents targeting multidrug-resistant bacteria and fungi. The antimicrobial efficacy of these compounds was assessed against a wide range of bacteria and fungi. Notably, derivatives **88**, and **89** (Fig. 28), exhibited significant antibacterial and antifungal properties, with more than half of the derivatives displaying superior minimum inhibitory concentration (MIC) values compared to the standard drugs used. Based on the structure–activity relationship (SAR) study, it is suggested that these bio-active molecules can be further improved as potent lead compounds

by incorporating additional electron-donating groups into the core structure. The presence of electron-donating groups such as hydroxy ( $-\text{OH}$ ) and methoxy ( $-\text{OCH}_3$ ) in the synthesized derivatives resulted in enhanced electron density, leading to the development of heterocyclic scaffolds with potent antibacterial and antifungal properties.

In an effort to enhance the antibacterial effects of chalcones and rhodanine-3-acetic acid, a series of hybrid compounds containing both chalcone and rhodanine-3-acetic acid components were synthesized by Z.-H. Chen *et al.*<sup>122</sup> and evaluated for their antibacterial activity. The antibacterial activities of these compounds were tested against both Gram-positive and Gram-negative bacteria, with a particular focus on multidrug-resistant strains of clinical isolates. Most of the synthesized compounds exhibited promising antibacterial activities, particularly against Gram-positive bacteria, including multidrug-resistant strains. Among the compounds tested, compound **90** (Fig. 28), demonstrated potent inhibitory capacity, with a minimum inhibitory concentration (MIC) of  $2 \text{ }\mu\text{g mL}^{-1}$ . This activity was comparable to that of the standard drug norfloxacin and slightly lower than that of oxacillin. These findings suggest that the hybrid compounds incorporating chalcone and rhodanine-3-acetic acid moieties may possess enhanced antibacterial properties while introduction of the acetamide group (compound **91**) in place of the halogens group significantly decreased the activity.

The analysis of chalcone derivatives highlights their promising antimicrobial properties, particularly against multidrug-resistant bacteria and fungi. The incorporation of ciprofloxacin into chalcone hybrids enhances their antibacterial activity, as evidenced by the reduced MIC values compared to ciprofloxacin alone. This suggests that the synergistic effects of chalcone and ciprofloxacin may offer a new approach for combating resistant bacterial strains. Additionally, the ability of these compounds to inhibit DNA gyrase further supports their potential as dual-action antibacterial agents. The derivatives mimicking cationic antimicrobial peptides show potent activity against a broad range of pathogens, including drug-resistant strains like MRSA. This is significant because it points to the ability of chalcones to bypass some resistance mechanisms that hinder traditional antibiotics. Furthermore, the incorporation of electron-donating substituents like methoxy and hydroxyl groups increases the antibacterial and anti-biofilm activity of chalcone derivatives. These findings indicate that careful structural modifications can enhance the potency and selectivity of chalcones. The hybridization approach, combining chalcones with other bioactive compounds such as rhodanine-3-acetic acid, demonstrates how combining different chemical entities can further improve antimicrobial activity.

## 5 Antiviral properties

The chalcone antiviral properties have also been investigated, showing potential in inhibiting the replication of certain viruses,<sup>123</sup> and in the search for development of antiviral agents, a series of chalcone derivatives containing a purine component were designed and synthesized by Gan, X., *et al.*<sup>124</sup> via



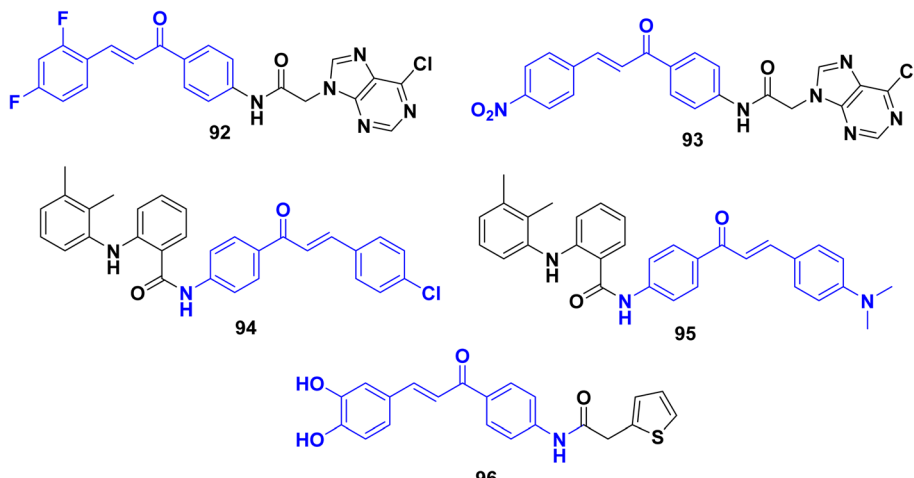


Fig. 29 Chalcone acetamides 92–96 with antiviral activity.

combining bioactive substructures. These derivatives were evaluated for their antiviral activity against tobacco mosaic virus (TMV) and cucumber mosaic virus (CMV). The results revealed that most of the derivatives exhibited antiviral properties. Notably, compounds 92 and 93 (Fig. 29), demonstrated excellent curative, protective, and inactivation activities against TMV. Their effective concentration values ( $EC_{50}$ ) were 452.4, 416.2, 241.2, and 438.7, 418.6, 261.7  $\mu\text{g mL}^{-1}$ , respectively, surpassing those of the reference drug ribavirin (585.8, 436.0, and 268.7  $\mu\text{g mL}^{-1}$ ). Furthermore, compounds 92 and 93 displayed remarkable curative and protective activities against CMV. Compound 92 exhibited moderate affinity for the TMV coat protein, with binding constants ( $K_a$ ) and dissociation constants ( $K_d$ ) of  $1.5 \times 10^4 \text{ L mol}^{-1}$  and  $79.8 \mu\text{mol L}^{-1}$ , respectively. These findings not only provide valuable insights into the structural aspects for the design of highly potent chalcone derivatives.

Al-Hazam *et al.*<sup>125</sup> synthesized a series of substituted chalcone-incorporated amide derivatives of mefenamic acid through the Claisen–Schmidt reaction with the aim of developing HIV non-nucleoside reverse transcriptase inhibitors. Additionally, two thiopyrimidine analogues were prepared. The compounds were evaluated for their inhibitory activity against HIV-1 and HIV-2. The synthesis involved the coupling of mefenamic acid with 4-amino-acetophenone, resulting in the formation of 4-(acetylphenyl)-2-((2,3-dimethylphenyl)amino)benzamide. Further condensation reactions with various substituted benzaldehydes led to the synthesis of substituted chalcone-incorporated amide derivatives. The synthesized compounds were then tested for their inhibitory activity against HIV-1 and HIV-2 using MT-4 cells. Compounds 94 and 95 (Fig. 29), exhibited cytotoxicity with  $IC_{50}$  values of 2.17 and 2.06  $\mu\text{M}$ , respectively, against mock-infected MT-4 cells. These findings suggest that compounds 94 and 95 hold promise as potential antileukemic agents.

A series of caffeoyl-anilide derivatives were synthesized by Bodiwala *et al.*<sup>126</sup> as dual inhibitors targeting both HIV-1 integrase (IN) and cellular CCR5. The intermediate compound, 4-

amino-3,4-dihydroxychalcone. In cell-based anti-HIV assays, compound 96 (Fig. 29), demonstrated a lower  $EC_{50} = 0.9 \mu\text{M}$  and a better therapeutic index (TI) compared to AZT, a standard antiretroviral drug. Mechanistic investigations indicated that the synthesized compounds inhibited both the entry of CCR5-tropic viruses and the integration step of the virus life cycle. Hence, the anti-HIV activity of these inhibitors likely stems from their specificity towards both targets. Molecular modeling studies provided insights into the predicted conformations of the compounds and their interactions with key amino acid residues (HIV-1 IN: Thr66, His67, Gln148, Lys159, and  $\text{Mg}^{2+}$ ; CCR5: Ser160, Lys197, and Phe245) within the active sites. These interactions help explain the observed inhibitory effects of the compounds.

## 6 Antiprotozoal properties

With the aim of developing potent antileishmanial compounds, a medicinal chemistry-driven approach was employed by ref. 127 to synthesize scaffolds with common pharmacophoric features of dihydropyrimidine and chalcone. The design of these compounds was guided by the X-ray structure of pteridine reductase 1 (PTR1) from *Leishmania* major. Several dihydropyrimidine-based derivatives were synthesized, targeting specific.

Several derivatives of bis-chalcone were synthesized by Domínguez *et al.*<sup>128</sup> and characterized, and their antimalarial activities were evaluated. Most of the synthesized compounds showed mild to moderate susceptibilities against *Plasmodium berghei*, with compound 1,1-bis-[(3',4'-N-(urenylphenyl)-3",4",5"-trimethoxyphenyl)]-2-propen-1-one 97 exhibiting the highest activity. Compound 97 (Fig. 30), inhibited heme polymerization by  $87.05 \pm 0.77\%$  and demonstrated increased survival time, reduced parasitemia, and delayed progression of malaria in infected mice. Compound 97 was further evaluated for its inhibitory effects on globin hydrolysis using a trophozoite-rich extract. The compound effectively inhibited the degradation of hemoglobin, surpassing the control groups

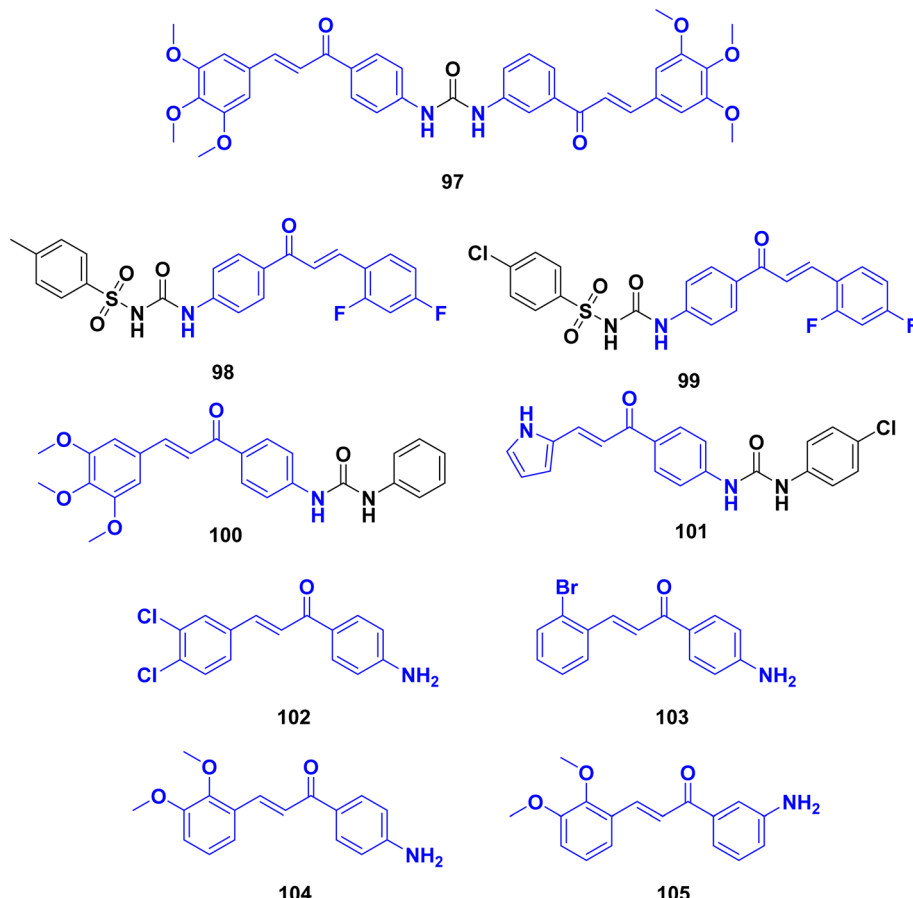


Fig. 30 Chalcone acetamides 97–105 with antiprotozoal activity.

(pepstatin and leupeptin). In an *in vivo* study using mice infected with *P. berghei*, compound 97 (administered at 20  $\mu$ g kg $^{-1}$ , ip once daily) and chloroquine (administered at 25 mg kg $^{-1}$ , ip once daily) were compared to a saline control group. Compound 97 significantly reduced parasitemia at the 4th day after infection compared to the control group. Moreover, compound 97 increased the survival time of infected mice, with deaths occurring between days 6 and 19 after infection, compared to the control group, where deaths occurred between days 9 and 11. While compound 97 showed the ability to reduce parasitemia and delay malaria progression, it did not completely eradicate the infection.

León, C., *et al.*<sup>129</sup> synthesized a series of sulfonylureas and evaluated for their antimalarial activities against *Plasmodium falciparum*. Compound 98 (Fig. 30), exhibited the highest activity with an IC<sub>50</sub> of 1.2  $\mu$ M against cultured *P. falciparum* parasites. The results suggest potent antimalarial activity for this compound, possibly through unknown mechanisms. Additionally, compound 99 also showed significant antimalarial effects with an IC<sub>50</sub> value of 2.1  $\mu$ M and demonstrated activity in a *P. berghei* mouse model, reducing parasitemia by 77% and increasing survival. The presence of 2,4-difluoro substitution in the aromatic ring of the  $\alpha,\beta$ -unsaturated ketone system was found to be important for mediating activity against *P. falciparum*. The fluorine substitution likely enhances

chemical interactions with the biological substrate. The results indicate that compound (98) inhibits hemoglobin degradation and hemozoin formation, contributing to its antimalarial activity *in vitro*. The findings also suggest that sulfonylurea derivatives with fluorine substitution in the aromatic ring maintain antimalarial efficacy *in vitro* and moderate activity *in vivo*, possibly due to electronic effects. The synthesized sulfonylurea compounds demonstrated antimalarial activity against *P. falciparum*. Compound (98) exhibited the highest potency, inhibiting parasite growth in cultured cells and reducing parasitemia in a mouse model. The presence of 2,4-difluoro substitution in the aromatic ring was crucial for mediating activity against *P. falciparum*. These findings contribute to the understanding of the antimalarial potential of sulfonylurea derivatives and suggest that compound (98) holds promise as a potential antimalarial compound.

Domínguez *et al.*<sup>130</sup> synthesized phenylurenyl chalcone derivatives and evaluated for their antimalarial properties against *Plasmodium falciparum*. Compound 100 (Fig. 30), showed the highest activity, with an IC<sub>50</sub> of 1.76  $\mu$ M against cultured *P. falciparum* parasites. Several other chalcone derivatives also exhibited significant antimalarial effects, both *in vitro* and in a murine malaria model. Compound 101 demonstrated good antimalarial activity *in vitro* and *in vivo*. It exhibited inhibitory effects on heme detoxification (89.2% inhibition) and



globin hydrolysis (98.64% inhibition). This compound contained an aromatic pyridinyl group, resembling the nitrogen of chloroquine, which may concentrate in the food vacuoles of malaria parasites. The relationship between antiparasitic activity, hemozoin formation inhibition, and hemoglobin hydrolysis was observed, indicating that potent inhibition of heme formation and hemoglobin hydrolysis does not guarantee antimalarial activity. Based on the data, compound **100** had the best antimalarial properties, inhibiting the development of *P. falciparum* in culture ( $IC_{50}$  of 1.76  $\mu$ M) and reducing parasitemia in *P. berghei* infected mice (from 23% to 6.8%). However, its mechanism of action does not appear to be related to hemoglobin hydrolysis or heme detoxification.

Jiang *et al.*<sup>131</sup> synthesized chalcone derivatives and investigated as potential anti-*Toxoplasma* agents. The compounds and evaluated for their anti-*Toxoplasma* activity *in vitro* and *in vivo*. The results demonstrated that several chalcone derivatives exhibited potent anti-*Toxoplasma* activity with low toxicity. Using the drug-food-homologous chalcone skeleton as a starting point, six series of chalcone derivatives were designed and synthesized. Approximately half of these compounds showed good anti-*Toxoplasma* activity *in vitro*. A quantitative structure-activity relationship (QSAR) model was established, indicating the significance of the Michael receptor in the chalcone molecular skeleton for enhancing activity. Four chalcone derivatives displayed potent anti-*T. gondii* activity and low cytotoxicity *in vitro*. *In vivo* studies revealed that three of these compounds **102**, **103**, and **105** (Fig. 30), effectively inhibited the proliferation of *Toxoplasma* tachyzoites. Moreover, these compounds exhibited liver-protecting effects, as evidenced by reduced liver and spleen index, as well as decreased levels of biochemical parameters associated with liver function. These findings suggest that these chalcone derivatives have protective effects on the liver of mice infected with *Toxoplasma* tachyzoites. The second study further supported the anti-*Toxoplasma* activity of chalcone derivatives. A QSAR model was established, confirming the importance of the Michael acceptor for their anti-*Toxoplasma* activity. Four compounds (**102**, **103**, **104**, and **105**) demonstrated potent activity against *T. gondii* *in vitro* while exhibiting low toxicity towards host cells.

## 7 Anti-inflammatory and antioxidant activity

The anti-inflammatory properties of chalcones arise from their ability to modulate key molecular targets and signaling pathways involved in the inflammatory response. Through various mechanisms, chalcones exhibit remarkable anti-inflammatory effects, making them promising candidates for the development of anti-inflammatory agents.<sup>132</sup> One of the primary mechanisms through which chalcones exert their anti-inflammatory effects is by inhibiting the activity of enzymes responsible for the production of inflammatory mediators. By targeting cyclooxygenase (COX) and lipoxygenase (LOX) enzymes, chalcones can impede the synthesis of prostaglandins and leukotrienes, respectively, thereby reducing the production

of these pro-inflammatory mediators. Furthermore, chalcones have been shown to suppress the expression and release of pro-inflammatory cytokines. These small proteins, such as tumor necrosis factor-alpha (TNF- $\alpha$ ), interleukin-1 beta (IL-1 $\beta$ ), and interleukin-6 (IL-6), play critical roles in orchestrating the inflammatory response. Chalcones can modulate the transcriptional activity of key transcription factors, such as nuclear factor-kappa B (NF- $\kappa$ B) and activator protein-1 (AP-1), leading to the downregulation of pro-inflammatory cytokine production. In addition to their impact on enzymes and cytokines, chalcones exhibit antioxidant properties.<sup>133</sup> By scavenging reactive oxygen species (ROS), chalcones can mitigate oxidative stress, a hallmark of inflammation. Oxidative stress can propagate inflammatory damage, and the antioxidant activity of chalcones helps to counteract this phenomenon, protecting cells from oxidative injury.<sup>134</sup> Moreover, chalcones modulate various signaling pathways implicated in inflammation, they can interfere with the activation of mitogen-activated protein kinases (MAPKs) and the phosphoinositide 3-kinase (PI3K)/Akt pathway, thereby regulating the expression of inflammatory genes. Through these actions, chalcones attenuate the inflammatory response at the molecular level.<sup>135</sup>

A series of trimethoxy phenyl-containing chalcone derivatives, pyrazoline derivatives, and pyrazole derivatives were synthesized by Abdelall, Lamie *et al.*<sup>136</sup> and evaluated for their COX-2 inhibitory activity, anti-inflammatory activity, histopathological effects. The compounds exhibited promising results in various assays. The synthesized compounds demonstrated selective COX-2 inhibitory activity, with higher potency against COX-2 compared to COX-1. Compound **106** (Fig. 31), displayed the most potent COX-2 inhibitory activity ( $IC_{50}$  = 0.039  $\mu$ M), surpassing that of the reference drug celecoxib ( $IC_{50}$  = 0.045  $\mu$ M), and exhibited a selectivity index value of 321.28, similar to celecoxib (S.I. = 326.66). Additionally, derivatives **107**, exhibited excellent COX-2 inhibitory activity ( $IC_{50}$  = 0.041–0.049  $\mu$ M) compared to celecoxib, with selectivity index values ranging from 230.61 to 278.05. In terms of anti-inflammatory activity, several compounds demonstrated prolonged inhibition of inflammation in an *in vivo* model, with inhibition percentages ranging from 33.21% to 44.52% after 7 hours following carrageenan injection.

A hit-to-lead effort was conducted by Zhang *et al.*<sup>137</sup> to discover and optimize NLRP3 inflammasome inhibitors. The research led to the identification of a potent lead compound **108** (Fig. 31), which exhibited improved inhibitory potency and minimal toxicity. Mechanistic investigations revealed that compound **108** suppressed NLRP3 inflammasome activation by inhibiting ROS production. Furthermore, treatment with compound **108** showed remarkable therapeutic effects in sepsis and colitis models induced by LPS and DSS, respectively. These findings encourage further development of more potent inhibitors based on the chemical scaffold of compound **108** and provide a valuable chemical tool for identifying its cellular binding target. During the study, a clinical compound library screen was utilized to identify elafibrinor (GFT505) as a NLRP3 inflammasome inhibitor with good safety. The chalcone pharmacophore of GFT505 was subjected to optimization through



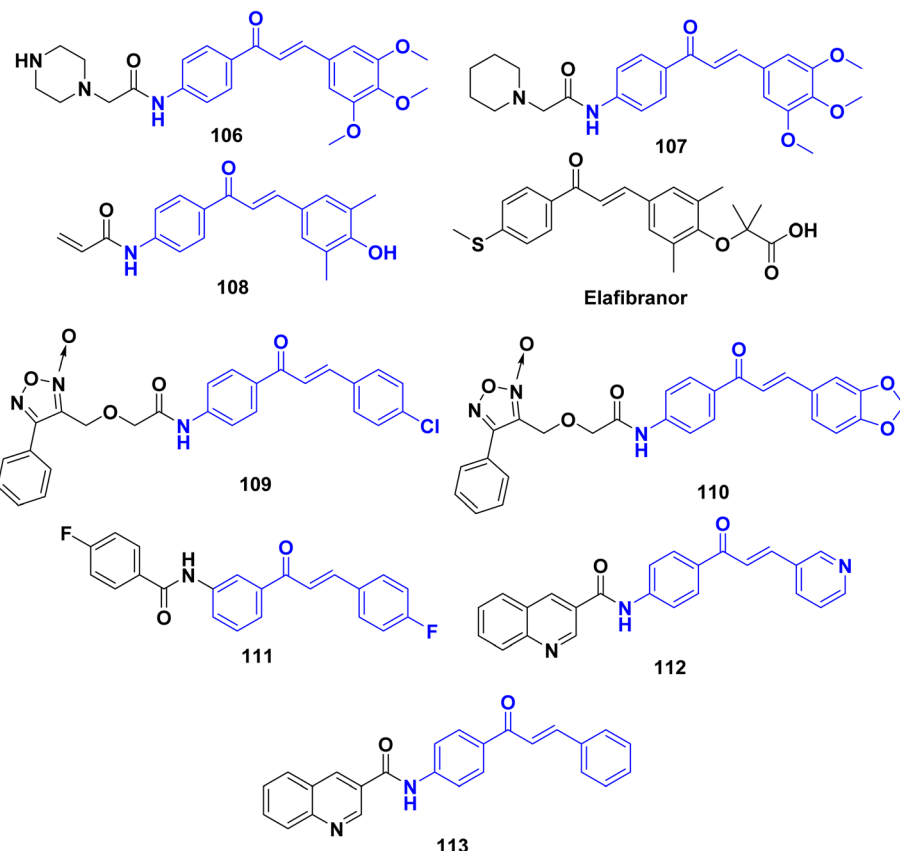


Fig. 31 Chalcone acetamides 106–113 with anti-inflammatory activity

structure–activity relationship (SAR) studies. By employing both simplification and replacement strategies guided by SAR and structure information, the researchers achieved enhancements in inhibitory activity. Notably, modifications that included the removal of a carboxyisopropyl moiety and the presence of suitable hydrogen bond donors at specific positions significantly improved the potency of the compound. Further exploration revealed that the 3,5-dimethyl moiety in the phenol group was crucial for potent inhibition of NLRP3 inflammasome activation. Subsequent modifications on the methylthio moiety resulted in the discovery of compound **108**, which exhibited approximately 30 times greater potency against NLRP3 inflammasome activation and lower toxicity compared to GFT505 at the cellular level. Compound **108** demonstrated favorable drug-like properties and showed efficacy in sepsis and colitis models. Ongoing chemoproteomic studies are aimed at identifying the cellular binding target of compound **108**. Collectively, these findings from a single study support the potential of compound **108** as a promising lead compound for NLRP3 inhibitors. The research highlights its therapeutic potential for inflammation and related diseases, while also providing insights into its mechanism of action and opportunities for further chemical development and investigation of its pharmacological properties.

A group of chalcone derivatives with nitric oxide (NO) donating properties were synthesized by Abuo-Rahma *et al.*,<sup>138</sup> and evaluated for their anti-inflammatory and gastroprotective

activities. The compounds were prepared by incorporating different NO donating moieties, including nitrate ester, oximes, and furoxans, into amino chalcones. The synthesized compounds demonstrated significant anti-inflammatory activity when tested using the carrageenan-induced rat paw edema method. Compared to the reference drug indomethacin, most of the prepared compounds exhibited higher levels of protection against inflammation. Moreover, the compounds showed a decreased incidence of gastric toxicity compared to indomethacin, as confirmed by histopathological investigation, which revealed reduced ulcer formation. The incorporation of NO-donating groups into the parent chalcone derivatives resulted in a moderate increase in anti-inflammatory activity and a marked decrease in gastric ulcerations compared to their parent chalcone derivatives. Notably, compounds, **109**, and **110** (Fig. 31), demonstrated the strongest anti-inflammatory activity among the synthesized compounds, with edema inhibition percentages of, 75%, and 72%, respectively, after 4 hours. These values corresponded to, 91%, and 87% of the activity exhibited by indomethacin. Additionally, the NO-donating furoxans exhibited the highest amount of NO release among the synthesized NO-donating hybrids. The prepared chalcone/NO hybrids, regardless of the NO donating moiety (nitrate ester, oxime, or furoxan), demonstrated pronounced gastroprotective activity, likely attributed to the release of NO. Histopathological examination further supported the reduction in gastric ulceration incidence due to the presence of the NO donating moiety.

J. Chu *et al.*<sup>139</sup> synthesized a group of chalcone derivatives and were evaluated for their antioxidant and anti-inflammatory activities, specifically targeting hepatic fibrosis patients. In terms of antioxidant activity, the chalcone derivatives demonstrated significant radical scavenging abilities, as determined by various methods such as H<sub>2</sub>O<sub>2</sub>, DPPH, ferrous reducing power, and nitric oxide assays. These compounds exhibited considerable efficacy in scavenging free radicals, indicating their potential as antioxidant agents. Furthermore, the synthesized chalcone derivatives were assessed for their anti-inflammatory activity by evaluating their inhibitory potency against NF- $\kappa$ B activation induced by LPS. The results revealed that all of the compounds efficiently inhibited the NF- $\kappa$ B activation provoked by LPS. Among the series, compound 111 (Fig. 31), was identified as the most potent inhibitor of NF- $\kappa$ B, displaying a relative NF- $\kappa$ B activity of  $1.12 \pm 0.53$ . Additionally, this compound exhibited inhibitory effects on various inflammatory mediators, including TNF- $\alpha$ , IL-1 $\beta$ , IL-6, and PGE2. The developed chalcone derivatives not only exhibited excellent antioxidant activity but also demonstrated considerable inhibitory activity against NF- $\kappa$ B, a key regulator of inflammation. Combined with their favorable dock score, these compounds hold promise as lead molecules for future drug discovery initiatives aimed at treating liver cirrhosis and hepatic fibrosis patients.

A series of quinoline linked chalcones derivatives were synthesized by Polo *et al.*<sup>140</sup> and evaluated for their inhibitory activity against acetylcholinesterase (AChE) and their anti-oxidative properties. Several compounds demonstrated selectivity against AChE, with compounds 112, and 113 (Fig. 31), exhibiting significant *in vitro* activity, displaying IC<sub>50</sub> values of 7.50, and 12.58  $\mu$ M, respectively. Compound 112 was identified as the most potent AChE inhibitor, with an IC<sub>50</sub> value of 7.50  $\mu$ M.

## 8 Conclusion and future directions

Chalcone-linked acetamide derivatives exhibit a remarkable array of biological activities, positioning them as promising candidates for therapeutic applications. The detailed exploration of their synthesis methods reveals innovative approaches that enhance the efficiency and scalability of these compounds. Through extensive analysis, it is evident that these derivatives possess potent antiproliferative properties, targeting critical pathways such as EGFR, topoisomerase I and II, ABCG2, caspase proteins, and histone deacetylase (HDAC), alongside their ability to inhibit tubulin polymerization. The elucidation of structure-activity relationships further underscores their potential as anticancer agents. In addition to their antiproliferative effects, chalcone-linked acetamide derivatives demonstrate significant antimicrobial, antiviral, and anti-protozoal properties, highlighting their versatility in combating a wide range of pathogens. Their robust anti-inflammatory and antioxidant activities further contribute to their therapeutic promise. The comprehensive evaluation of these bioactivities suggests that chalcone-linked acetamide derivatives are valuable candidates for drug discovery and development.

## Data availability

No new data were created or analyzed during this study. Data sharing is not applicable to this article.

## Conflicts of interest

The authors declare that there is no conflict of interest.

## References

- 1 S.-X. Lin, J. Chen, M. Mazumdar, D. Poirier, C. Wang, A. Azzi and M. Zhou, *Nat. Rev. Endocrinol.*, 2010, **6**, 485–493.
- 2 D. K. Mahapatra, S. K. Bharti and V. Asati, *Eur. J. Med. Chem.*, 2015, **98**, 69–114.
- 3 L. H. Cazarolli, V. D. Kappel, A. P. Zanatta, D. O. H. Suzuki, R. A. Yunes, R. J. Nunes, M. G. Pizzolatti and F. R. M. B. Silva, *Stud. Nat. Prod. Chem.*, 2013, **39**, 47–89.
- 4 B. Zhou and C. Xing, *Med. Chem.*, 2015, **5**, 388.
- 5 C. Karthikeyan, N. S. H. Narayana Moorthy, S. Ramasamy, U. Vanam, E. Manivannan, D. Karunagaran and P. Trivedi, *Recent Pat. Anti-Cancer Drug Discovery*, 2015, **10**, 97–115.
- 6 A. Boumendjel, X. Ronot and J. Boutonnat, *Curr. Drug Targets*, 2009, **10**, 363–371.
- 7 A. J. Leon-Gonzalez, N. Acero, D. Muñoz-Mingarro, I. Navarro and C. Martín-Cordero, *Curr. Med. Chem.*, 2015, **22**, 3407–3425.
- 8 D. K. Mahapatra, V. Asati and S. K. Bharti, *Eur. J. Med. Chem.*, 2015, **92**, 839–865.
- 9 D. K. Mahapatra and S. K. Bharti, *Life Sci.*, 2016, **148**, 154–172.
- 10 C. Zhuang, W. Zhang, C. Sheng, W. Zhang, C. Xing and Z. Miao, *Chem. Rev.*, 2017, **117**, 7762–7810.
- 11 D. Kumar, M. Kumar, A. Kumar and S. Kumar Singh, *Mini-Rev. Med. Chem.*, 2013, **13**, 2116–2133.
- 12 A. Hameed, M. I. Abdullah, E. Ahmed, A. Sharif, A. Irfan and S. Masood, *Bioorg. Chem.*, 2016, **65**, 175–182.
- 13 Z. Wan, D. Hu, P. Li, D. Xie and X. Gan, *Molecules*, 2015, **20**, 11861–11874.
- 14 F. Peng, Q. Du, C. Peng, N. Wang, H. Tang, X. Xie, J. Shen and J. Chen, *Phytother. Res.*, 2015, **29**, 969–977.
- 15 J.-Y. Kim, S. J. Park, K.-J. Yun, Y.-W. Cho, H.-J. Park and K.-T. Lee, *Eur. J. Pharmacol.*, 2008, **584**, 175–184.
- 16 E. Oledzka, *Int. J. Mol. Sci.*, 2024, **25**, 3398.
- 17 M. Yang, N. Li, F. Li, Q. Zhu, X. Liu, Q. Han, Y. Wang, Y. Chen, X. Zeng and Y. Lv, *Int. Immunopharmacol.*, 2013, **16**, 466–474.
- 18 M. Liu, P. E. Hansen, G. Wang, L. Qiu, J. Dong, H. Yin, Z. Qian, M. Yang and J. Miao, *Molecules*, 2015, **20**, 754–779.
- 19 S. C. Narayananpillai, P. Leitzman, M. G. O'Sullivan and C. Xing, *Chem. Res. Toxicol.*, 2014, **27**, 1871–1876.
- 20 B. Das, A. T. Baidya, A. T. Mathew, A. K. Yadav and R. Kumar, *Bioorg. Med. Chem.*, 2022, **56**, 116614.
- 21 S. Mahesh, K.-C. Tang and M. Raj, *Molecules*, 2018, **23**, 2615.



22 Z. Chen, H. Luo, A. Gubu, S. Yu, H. Zhang, H. Dai, Y. Zhang, B. Zhang, Y. Ma and A. Lu, *Front. Cell Dev. Biol.*, 2023, **11**, 1091809.

23 V. S. Gontijo, F. P. D. Viegas, C. J. Ortiz, M. de Freitas Silva, C. M. Damasio, M. C. Rosa, T. G. Campos, D. S. Couto, K. S. Tranches Dias and C. Viegas, *Curr. Neuropharmacol.*, 2020, **18**, 348–407.

24 S. Shukla, A. K. Sood, K. Goyal, A. Singh, V. Sharma, N. Guliya, S. Gulati and S. Kumar, *Anti-Cancer Agents Med. Chem.*, 2021, **21**, 1650–1670.

25 G. B. Souza, T. A. Santos, A. P. Silva, A. L. S. Barreiros, V. B. Nardelli, I. B. Siqueira, S. S. Dolabella, E. V. Costa, P. B. Alves and R. Scher, *Nat. Prod. Res.*, 2022, 1–8.

26 S. Nasir Abbas Bukhari, M. Jasamai, I. Jantan and W. Ahmad, *Mini-Rev. Org. Chem.*, 2013, **10**, 73–83.

27 S. A. Khan, A. M. Asiri, N. S. M. Al-Ghamdi, M. Asad, M. E. Zayed, S. A. Elroby, F. M. Aqlan, M. Y. Wani and K. Sharma, *J. Mol. Struct.*, 2019, **1190**, 77–85.

28 T. Narender and K. P. Reddy, *Tetrahedron Lett.*, 2007, **48**, 3177–3180.

29 M. Al-Masum, E. Ng and M. C. Wai, *Tetrahedron Lett.*, 2011, **52**, 1008–1010.

30 S. Nasir Abbas Bukhari, M. Jasamai and I. Jantan, *Mini-Rev. Med. Chem.*, 2012, **12**, 1394–1403.

31 M. M. Heravi, V. Zadsirjan, P. Saedi and T. Momeni, *RSC Adv.*, 2018, **8**, 40061–40163.

32 A. Scettri, R. Villano and M. R. Acocella, *Molecules*, 2009, **14**, 3030–3036.

33 A. Kumar, S. Sharma, V. D. Tripathi and S. Srivastava, *Tetrahedron*, 2010, **66**, 9445–9449.

34 M. Haddach and J. R. McCarthy, *Tetrahedron Lett.*, 1999, **40**, 3109–3112.

35 S. Eddarir, N. Cotelle, Y. Bakkour and C. Rolando, *Tetrahedron Lett.*, 2003, **44**, 5359–5363.

36 D. Wu and C. Prives, *Cell Death Differ.*, 2018, **25**, 169–179.

37 A. Kamal, G. B. Kumar, M. Vishnuvardhan, A. B. Shaik, V. S. Reddy, R. Mahesh, I. B. Sayeeda and J. S. Kapure, *Org. Biomol. Chem.*, 2015, **13**, 3963–3981.

38 V. R. Yadav, S. Prasad, B. Sung and B. B. Aggarwal, *Int. Immunopharmacol.*, 2011, **11**, 295–309.

39 M. J. Mphahlele, M. M. Maluleka, N. Parbhoo and S. T. Malindisa, *Int. J. Mol. Sci.*, 2018, **19**, 2552.

40 L. Wang, G. Chen, X. Lu, S. Wang, S. Han, Y. Li, G. Ping, X. Jiang, H. Li and J. Yang, *Eur. J. Med. Chem.*, 2015, **89**, 88–97.

41 J. H. Jeong, H. J. Jang, S. Kwak, G. J. Sung, S. H. Park, J. H. Song, H. Kim, Y. Na and K. C. Choi, *J. Cell. Biochem.*, 2019, **120**, 977–987.

42 Z. Parveen, G. Brunhofer, I. Jabeen, T. Erker, P. Chiba and G. F. Ecker, *Bioorg. Med. Chem.*, 2014, **22**, 2311–2319.

43 I. K. Lindamulage, H.-Y. Vu, C. Karthikeyan, J. Knockleby, Y.-F. Lee, P. Trivedi and H. Lee, *Sci. Rep.*, 2017, **7**, 10298.

44 E. Winter, P. c. Devantier Neuenfeldt, L. D. Chiaradia-Delatorre, C. Gauthier, R. A. Yunes, R. J. Nunes, T. n. B. Creczynski-Pasa and A. Di Pietro, *J. Med. Chem.*, 2014, **57**, 2930–2941.

45 Y. Ouyang, J. Li, X. Chen, X. Fu, S. Sun and Q. Wu, *Biomolecules*, 2021, **11**, 894.

46 T. Zubair and D. Bandyopadhyay, *Int. J. Mol. Sci.*, 2023, **24**, 2651.

47 P. Wee and Z. Wang, *Cancers*, 2017, **9**, 52.

48 P. Seshacharyulu, M. P. Ponnusamy, D. Haridas, M. Jain, A. K. Ganti and S. K. Batra, *Expert Opin. Ther. Targets*, 2012, **16**, 15–31.

49 W.-Q. Cai, L.-S. Zeng, L.-F. Wang, Y.-Y. Wang, J.-T. Cheng, Y. Zhang, Z.-W. Han, Y. Zhou, S.-L. Huang and X.-W. Wang, *Front. Oncol.*, 2020, **10**, 1249.

50 S. Kumagai, S. Koyama and H. Nishikawa, *Nat. Rev. Cancer*, 2021, **21**, 181–197.

51 X. Du, B. Yang, Q. An, Y. G. Assaraf, X. Cao and J. Xia, *Innovation*, 2021, **2**(2), 100103.

52 A. M. Mohassab, H. A. Hassan, D. Abdelhamid, A. M. Gouda, B. G. Youssif, H. Tateishi, M. Fujita, M. Otsuka and M. Abdel-Aziz, *Bioorg. Chem.*, 2021, **106**, 104510.

53 M. A. A. Fathi, A. A. Abd El-Hafeez, D. Abdelhamid, S. H. Abbas, M. M. Montano and M. Abdel-Aziz, *Bioorg. Chem.*, 2019, **84**, 150–163.

54 H. A. Abou-Zied, B. G. Youssif, M. F. Mohamed, A. M. Hayallah and M. Abdel-Aziz, *Bioorg. Chem.*, 2019, **89**, 102997.

55 M. Hisham, H. A. Hassan, H. A. Gomaa, B. G. Youssif, A. M. Hayallah and M. Abdel-Aziz, *J. Mol. Struct.*, 2022, **1254**, 132422.

56 H. A. Abou-Zied, E. A. Beshr, H. A. Gomaa, Y. A. Mostafa, B. G. Youssif, A. M. Hayallah and M. Abdel-Aziz, *Arch. Pharm.*, 2022, e2200464.

57 F. F. Hagar, S. H. Abbas, D. Abdelhamid, H. A. Gomaa, B. G. Youssif and M. Abdel-Aziz, *Arch. Pharm.*, 2023, **356**, 2200357.

58 M. S. Abdelbasset, M. Abdel-Aziz, M. Ramadan, M. H. Abdelrahman, S. N. A. Bukhari, T. F. Ali and G. E.-D. A. Abuo-Rahma, *Bioorg. Med. Chem.*, 2019, **27**, 1076–1086.

59 M. T. E. Maghraby, O. I. Salem, B. G. Youssif and M. M. Sheha, *Chem. Biol. Drug Des.*, 2023, **101**, 749–759.

60 X. Liang, Q. Wu, S. Luan, Z. Yin, C. He, L. Yin, Y. Zou, Z. Yuan, L. Li and X. Song, *Eur. J. Med. Chem.*, 2019, **171**, 129–168.

61 W. A. Denny, *Expert Opin. Emerging Drugs*, 2004, **9**, 105–133.

62 H. H. Mohammed, S. H. Abbas, A. M. Hayallah, G. E.-D. A. Abuo-Rahma and Y. A. Mostafa, *Bioorg. Chem.*, 2021, **106**, 104422.

63 S.-H. Kim, E. Lee, K. H. Baek, H. B. Kwon, H. Woo, E.-S. Lee, Y. Kwon and Y. Na, *Bioorg. Med. Chem. Lett.*, 2013, **23**, 3320–3324.

64 M. Abdel-Aziz, S.-E. Park, G. E.-D. A. Abuo-Rahma, M. A. Sayed and Y. Kwon, *Eur. J. Med. Chem.*, 2013, **69**, 427–438.

65 K. P. Locher, *Nat. Struct. Mol. Biol.*, 2016, **23**, 487–493.

66 Q. Mao and J. D. Unadkat, *AAPS J.*, 2015, **17**, 65–82.

67 I. F. Zattoni, L. C. Delabio, J. de Paula Dutra, D. H. Kita, G. Scheiffer, M. Hembecker, G. da Silva Pereira,



V. R. Moure and G. Valdameri, *Eur. J. Med. Chem.*, 2022, **237**, 114346.

68 Y. Toyoda, T. Takada and H. Suzuki, *Front. Pharmacol.*, 2019, **10**, 208.

69 S. Kukal, D. Guin, C. Rawat, S. Bora, M. K. Mishra, P. Sharma, P. R. Paul, N. Kanojia, G. K. Grewal and S. Kukreti, *Cell. Mol. Life Sci.*, 2021, 1–53.

70 S. Kraege, S. C. Köhler and M. Wiese, *ChemMedChem*, 2016, **11**, 2422–2435.

71 S. Kraege, K. Stefan, S. C. Köhler and M. Wiese, *ChemMedChem*, 2016, **11**, 2547–2558.

72 K. Juvale, V. F. Pape and M. Wiese, *Bioorg. Med. Chem.*, 2012, **20**, 346–355.

73 A. B. Parrish, C. D. Freel and S. Kornbluth, *Cold Spring Harbor Perspect. Biol.*, 2013, **5**, a008672.

74 G. Pistrutto, D. Trisciuglio, C. Ceci, A. Garufi and G. D’Orazi, *Aging*, 2016, **8**, 603.

75 S. H. MacKenzie, J. L. Schipper and A. C. Clark, *Curr. Opin. Drug Discovery Dev.*, 2010, **13**, 568.

76 S. Hashem, T. A. Ali, S. Akhtar, S. Nisar, G. Sageena, S. Ali, S. Al-Mannai, L. Therachiyl, R. Mir and I. Elfaki, *Biomed. Pharmacother.*, 2022, **150**, 113054.

77 M. Vizovisek, D. Ristanovic, S. Menghini, M. G. Christiansen and S. Schuerle, *Int. J. Mol. Sci.*, 2021, **22**, 2514.

78 J. Murray and A. R. Renslo, *Curr. Opin. Struct. Biol.*, 2013, **23**, 812–819.

79 F. Tok, B. İ. Abas, Ö. Çevik and B. Koçyiğit-Kaymakçıoğlu, *Bioorg. Chem.*, 2020, **102**, 104063.

80 F. F. Ahmed, A. A. Abd El-Hafeez, S. H. Abbas, D. Abdelhamid and M. Abdel-Aziz, *Eur. J. Med. Chem.*, 2018, **151**, 705–722.

81 R. Romagnoli, P. G. Baraldi, M. D. Carrion, O. Cruz-Lopez, C. L. Cara, J. Balzarini, E. Hamel, A. Canella, E. Fabbri and R. Gambari, *Bioorg. Med. Chem. Lett.*, 2009, **19**, 2022–2028.

82 Y. Li and E. Seto, *Cold Spring Harbor Perspect. Med.*, 2016, **6**, a026831.

83 S. Patra, D. P. Panigrahi, P. P. Praharaj, C. S. Bhol, K. K. Mahapatra, S. R. Mishra, B. P. Behera, M. Jena and S. K. Bhutia, *Cell. Mol. Life Sci.*, 2019, **76**, 3263–3282.

84 H. P. Chen, Y. T. Zhao and T. C. Zhao, *Crit. Rev. Oncog.*, 2015, **20**(1–2), 35–47.

85 M. Dickinson, R. W. Johnstone and H. M. Prince, *Invest. New Drugs*, 2010, **28**, 3–20.

86 P. Chun, *Arch. Pharmacal Res.*, 2015, **38**, 933–949.

87 S. Valente, D. Trisciuglio, M. Tardugno, R. Benedetti, D. Labella, D. Secci, C. Mercurio, R. Boggio, S. Tomassi and S. Di Maro, *ChemMedChem*, 2013, **8**, 800–811.

88 A. A. Mourad, M. A. Mourad and P. G. Jones, *Drug Des., Dev. Ther.*, 2020, 3111–3130.

89 M. Knossow, V. Campanacci, L. A. Khodja and B. Gigant, *iScience*, 2020, **23**(9), 101511.

90 W. Liu, M. He, Y. Li, Z. Peng and G. Wang, *J. Enzyme Inhib. Med. Chem.*, 2022, **37**, 9–38.

91 E. Mukhtar, V. M. Adhami and H. Mukhtar, *Mol. Cancer Ther.*, 2014, **13**, 275–284.

92 G. S. Karatoprak, E. Küpeli Akkol, Y. Genç, H. Bardakçı, C. Yücel and E. Sobarzo-Sánchez, *Molecules*, 2020, **25**, 2560.

93 M. M. Amin, G. E.-D. A. Abuo-Rahma, M. S. A. Shaykoon, A. A. Marzouk, M. A. Abourehab, R. E. Saraya, M. Badr, A. M. Sayed and E. A. Beshr, *Bioorg. Chem.*, 2023, **134**, 106444.

94 H. Del Rosario, E. Saavedra, I. Brouard, D. González-Santana, C. García, E. Spínola-Lasso, C. Tabraue, J. Quintana and F. Estévez, *Bioorg. Chem.*, 2022, **127**, 105926.

95 Y. Li, Y. Sun, Y. Zhou, X. Li, H. Zhang and G. Zhang, *J. Enzyme Inhib. Med. Chem.*, 2021, **36**, 207–217.

96 D.-J. Fu, J.-H. Li, J.-J. Yang, P. Li, Y.-B. Zhang, S. Liu, Z.-R. Li and S.-Y. Zhang, *Bioorg. Chem.*, 2019, **86**, 375–385.

97 P. F. Lamie and J. N. Philoppe, *J. Enzyme Inhib. Med. Chem.*, 2020, **35**, 864–879.

98 J.-L. Ren, X.-Y. Zhang, B. Yu, X.-X. Wang, K.-P. Shao, X.-G. Zhu and H.-M. Liu, *Eur. J. Med. Chem.*, 2015, **93**, 321–329.

99 M. A. Mourad, M. Abdel-Aziz, G. E.-D. A. Abuo-Rahma and H. H. Farag, *Eur. J. Med. Chem.*, 2012, **54**, 907–913.

100 X. Cao, R. Li, H. Xiong, J. Su, C. Guo, T. An, H. Zong and R. Zhao, *Eur. J. Med. Chem.*, 2021, **221**, 113520.

101 S. Patel, N. Challagundla, R. A. Rajput and S. Mishra, *Bioorg. Chem.*, 2022, **127**, 106036.

102 C.-F. Lu, S.-H. Wang, X.-J. Pang, T. Zhu, H.-L. Li, Q.-R. Li, Q.-Y. Li, Y.-F. Gu, Z.-Y. Mu and M.-J. Jin, *Molecules*, 2020, **25**, 5530.

103 P. N. Bandeira, T. L. G. Lemos, H. S. Santos, M. C. S. de Carvalho, D. P. Pinheiro, M. O. de Moraes Filho, C. Pessoa, F. W. A. Barros-Nepomuceno, T. H. S. Rodrigues and P. R. V. Ribeiro, *Med. Chem. Res.*, 2019, **28**, 2037–2049.

104 S. D. Durgapal, R. Soni, S. Umar, B. Suresh and S. S. Soman, *Chem. Biol. Drug Des.*, 2018, **92**, 1279–1287.

105 H. A. El-Sherief, G. E.-D. A. Abuo-Rahma, M. E. Shoman, E. A. Beshr and R. M. Abdel-baky, *Med. Chem. Res.*, 2017, **26**, 3077–3090.

106 A. M. Farrag, *Arch. Pharm.*, 2016, **349**, 904–914.

107 J. Rodrigues, C. Abramjuk, L. Vásquez, N. Gamboa, J. Domínguez, B. Nitzsche, M. Höpfner, R. Georgieva, H. Bäumler and C. Stephan, *Pharm. Res.*, 2011, **28**, 907–919.

108 H. Bhojwani, K. Begwani, V. Bhor, P. Bedi, N. Balasinor, S. Raut and U. Joshi, *Arch. Pharm.*, 2023, e2200405.

109 S. Lakshmanan, D. Govindaraj, K. Mahalakshmi, K. Thirumurugan, N. Ramalakshmi and S. A. Antony, *Struct. Chem.*, 2021, **32**, 1597–1609.

110 Y. Um, S. Cho, H. B. Woo, Y. K. Kim, H. Kim, J. Ham, S.-N. Kim, C. M. Ahn and S. Lee, *Bioorg. Med. Chem.*, 2008, **16**, 3608–3615.

111 V. R. Avupati, R. P. Yejella, G. Guntuku and P. Gunta, *Bioorg. Med. Chem. Lett.*, 2012, **22**, 1031–1035.

112 D. Chinemerem Nwobodo, M. C. Ugwu, C. Oliseloke Anie, M. T. Al-Ouqaili, J. Chinedu Ikem, U. Victor Chigozie and M. Saki, *J. Clin. Lab. Anal.*, 2022, **36**, e24655.

113 M. Ritter, R. Mastelari Martins, D. Dias and C. MP Pereira, *Lett. Org. Chem.*, 2014, **11**, 498–508.



114 S. Wang, C. Li, L. Zhang, B. Sun, Y. Cui and F. Sang, *Bioorg. Med. Chem.*, 2023, 117454.

115 F. Farhadi, B. Khameneh, M. Iranshahi and M. Iranshahy, *Phytother. Res.*, 2019, **33**, 13–40.

116 D. Gupta and D. Jain, *J. Adv. Pharm. Technol. Res.*, 2015, **6**, 114.

117 R. Irfan, S. Mousavi, M. Alazmi and R. S. Z. Saleem, *Molecules*, 2020, **25**, 5381.

118 H. H. Mohammed, D. M. E. Ali, M. Badr, A. G. Habib, A. M. Mahmoud, S. M. Farhan, S. S. H. A. E. Gany, S. A. Mohamad, A. M. Hayallah and S. H. Abbas, *Mol. Diversity*, 2023, **27**, 1751–1765.

119 W.-C. Chu, P.-Y. Bai, Z.-Q. Yang, D.-Y. Cui, Y.-G. Hua, Y. Yang, Q.-Q. Yang, E. Zhang and S. Qin, *Eur. J. Med. Chem.*, 2018, **143**, 905–921.

120 S. M. El-Messery, E.-S. E. Habib, S. T. Al-Rashood and G. S. Hassan, *J. Enzyme Inhib. Med. Chem.*, 2018, **33**, 818–832.

121 D. Joshi and K. S. Parikh, *Med. Chem. Res.*, 2014, **23**, 1855–1864.

122 Z.-H. Chen, C.-J. Zheng, L.-P. Sun and H.-R. Piao, *Eur. J. Med. Chem.*, 2010, **45**, 5739–5743.

123 D. Elkhalifa, I. Al-Hashimi, A.-E. Al Moustafa and A. Khalil, *J. Drug Targeting*, 2021, **29**, 403–419.

124 X. Gan, Y. Wang, D. Hu and B. Song, *Chin. J. Chem.*, 2017, **35**, 665–672.

125 H. A. Al-Hazam, Z. A. Al-Shamkani, N. A. Al-Masoudi, B. A. Saeed and C. Pannecouque, *Z. Naturforsch., B*, 2017, **72**, 249–256.

126 H. S. Bodiwala, S. Sabde, P. Gupta, R. Mukherjee, R. Kumar, P. Garg, K. K. Bhutani, D. Mitra and I. P. Singh, *Bioorg. Med. Chem.*, 2011, **19**, 1256–1263.

127 U. Rashid, R. Sultana, N. Shaheen, S. F. Hassan, F. Yaqoob, M. J. Ahmad, F. Iftikhar, N. Sultana, S. Asghar and M. Yasinzai, *Eur. J. Med. Chem.*, 2016, **115**, 230–244.

128 J. N. Domínguez, N. Gamboa de Domínguez, J. Rodrigues, M. E. Acosta, N. Caraballo and C. León, *J. Enzyme Inhib. Med. Chem.*, 2013, **28**, 1267–1273.

129 C. León, J. Rodrigues, N. G. de Domínguez, J. Charris, J. Gut, P. J. Rosenthal and J. N. Domínguez, *Eur. J. Med. Chem.*, 2007, **42**, 735–742.

130 J. N. Domínguez, C. León, J. Rodrigues, N. Gamboa de Domínguez, J. Gut and P. J. Rosenthal, *J. Med. Chem.*, 2005, **48**, 3654–3658.

131 L. Jiang, B. Liu, S. Hou, T. Su, Q. Fan, E. Alyafeai, Y. Tang, M. Wu, X. Liu and J. Li, *Eur. J. Med. Chem.*, 2022, **234**, 114244.

132 J. Wu, J. Li, Y. Cai, Y. Pan, F. Ye, Y. Zhang, Y. Zhao, S. Yang, X. Li and G. Liang, *J. Med. Chem.*, 2011, **54**, 8110–8123.

133 H. Inoue and R. Nakata, *Endocr., Metab. Immune Disord.: Drug Targets*, 2015, **15**, 186–195.

134 S. Dhakal, P. A. Ramsland, B. Adhikari and I. Macreadie, *Int. J. Mol. Sci.*, 2021, **22**, 9456.

135 Q. Fang, L. Deng, L. Wang, Y. Zhang, Q. Weng, H. Yin, Y. Pan, C. Tong, J. Wang and G. Liang, *J. Pharmacol. Exp. Ther.*, 2015, **355**, 235–246.

136 E. K. Abdelall, P. F. Lamie, L. S. Aboelnaga and R. M. Hassan, *Bioorg. Chem.*, 2022, **124**, 105806.

137 C. Zhang, H. Yue, P. Sun, L. Hua, S. Liang, Y. Ou, D. Wu, X. Wu, H. Chen and Y. Hao, *Eur. J. Med. Chem.*, 2021, **219**, 113417.

138 G. E.-D. A. Abuo-Rahma, M. Abdel-Aziz, M. A. Mourad and H. H. Farag, *Bioorg. Med. Chem.*, 2012, **20**, 195–206.

139 J. Chu and C. L. Guo, *Arch. Pharm.*, 2016, **349**, 63–70.

140 E. Polo, N. Ibarra-Arellano, L. Prent-Peñaloza, A. Morales-Bayuelo, J. Henao, A. Galdámez and M. Gutiérrez, *Bioorg. Chem.*, 2019, **90**, 103034.

